processes

MDPI

Review

Corn Residue-Based Activated Carbon for Heavy Metal Removal: A Review of Adsorptive Performance and Properties

Marina Radenković *, Marija Kovačević, Vuk Radojičić, Miloš Tošić, Miloš Momčilović and Sanja Živković *

Department of Physical Chemistry, VINČA Institute of Nuclear Sciences–National Institute of the Republic of Serbia, University of Belgrade, P.O. Box 522, 11000 Belgrade, Serbia; marija.kovacevic@vin.bg.ac.rs (M.K.); vuk.radojicic@vin.bg.ac.rs (V.R.); milos.tosic@vin.bg.ac.rs (M.T.); milos@vin.bg.ac.rs (M.M.)
* Correspondence: marinar@vin.bg.ac.rs (M.R.); sanjaz@vin.bg.ac.rs (S.Ž.)

Abstract

Corn (*Zea mays* L.) ranks among the most important cereal crops globally, extensively cultivated for food, animal feed, and industrial applications. Its large-scale production generates substantial amounts of agricultural residues such as cobs, husks, stalks, leaves and other, which are often underutilized, leading to environmental concerns. Due to their high carbon content, lignocellulosic structure, and abundant availability, these residues represent a sustainable and low-cost raw material for the synthesis of activated carbon. Corn waste-derived activated carbon has emerged as a promising material for the efficient removal of heavy metals from aqueous solutions. Its high surface area, well-developed porosity, and adjustable surface chemistry, referring to the functional groups on the adsorbent surface that can be modified to enhance affinity toward metal ions, facilitate effective adsorption. This review provides a comprehensive overview of (1) the potential of corn waste biomass as a precursor for activated carbon production, (2) methods of carbonization and activation that influence the textural and chemical properties of the resulting adsorbents, (3) adsorption performance for heavy metal removal under varying experimental parameters such as pH, initial concentration, contact time, and adsorbent dosage, (4) adsorption mechanisms responsible for heavy metal uptake. Reported maximum adsorption capacities vary for different metals, ranging from 2.814–206 mg/g for lead, 0.21–87.72 mg/g for cadmium, 9.6246–175.44 mg/g for chromium, and 0.724–643.92 mg/g for copper. Utilizing corn waste not only provides an eco-friendly approach for managing agricultural residues but also supports the development of efficient adsorbents. Nevertheless, challenges such as scaling up production and evaluating adsorbent performance in real wastewater samples remain and require further investigation. Finally, the review highlights key challenges and knowledge gaps in current research and offers recommendations for future studies aimed at advancing the practical application of corn waste–based activated carbons in water treatment.

Keywords: corn waste biomass; activated carbon; heavy metal; adsorption mechanisms

check for updates

Academic Editor: Anna Wołowicz

Received: 30 September 2025
Revised: 15 October 2025
Accepted: 21 October 2025
Published: 23 October 2025

Citation: Radenković, M.; Kovačević, M.; Radojičić, V.; Tošić, M.; Momčilović, M.; Živković, S. Corn Residue-Based Activated Carbon for Heavy Metal Removal: A Review of Adsorptive Performance and Properties. *Processes* **2025**, *13*, 3406. https://doi.org/10.3390/pr13113406

Copyright: © 2025 by the authors. Licensee MDPI, Basel, Switzerland. This article is an open access article distributed under the terms and conditions of the Creative Commons Attribution (CC BY) license (https://creativecommons.org/licenses/by/4.0/).

1. Introduction

Water pollution, a major aspect of environmental contamination, remains a pressing global issue. Wastewater contaminated with heavy metals, such as arsenic, cadmium, chromium, copper, mercury, iron, nickel, lead and zinc, generated by human activities

such as farming, industrial operations (e.g., mining, battery manufacturing, and textile production), and domestic wastewater discharge, presents significant risks to ecosystems and public health. Furthermore, heavy metals present in contaminated water can be assimilated by plants through bioaccumulation processes, subsequently infiltrating the food chain and causing adverse effects on human and animal health [1]. For example, lead exposure has been shown to cause toxic effects on the renal, gastrointestinal, central nervous, cardiovascular, and reproductive systems. Similarly, cadmium negatively affects the kidneys, heart, lungs, liver, and bones, while arsenic is linked to gastrointestinal disturbances and cardiorenal complications [2]. Given the well-documented evidence of heavy metal toxicity, coupled with the growing number of metal poisoning incidents, the preservation of safe and reliable drinking water sources has become a global priority. Consequently, the demand for effective treatment solutions for heavy metal-contaminated water is increasingly urgent [3]. Table 1 summarizes the investigated metals, their permissible limits in drinking water according to WHO, typical sources, health impacts, and relevant references. Various conventional methods, such as chemical precipitation, solvent extraction, ion exchange, electrochemical treatment, and membrane filtration, have been employed to remove heavy metals from water. However, these techniques are often ineffective at treating low concentrations of metals. To address the uncontrolled discharge of these hazardous pollutants, innovative and sustainable treatment technologies are being actively developed worldwide [4]. Among them, adsorption has emerged as a promising and efficient alternative, offering advantages such as low operational cost, design flexibility, and high removal efficiency even at trace concentrations of contaminants. Today, it is regarded as an efficient and superior method in comparison to traditional methods for heavy metal wastewater treatment, delivering high-quality treated effluent [5,6]. Table 2 summarizes the main advantages and limitations of these conventional treatment methods, as well as the adsorption process. While some of the used literature also covered other pollutants, both organic (methyl orange [7], methylene blue [8], tetracycline [9]) and inorganic (nitrates [9]), in this review, we focused on heavy metals and on providing a comprehensive overview of the subject.

Activated carbon is a highly porous carbon-based material with a large internal surface area, generally obtained from carbon-rich precursors by producing char through carbonization, followed by activation using oxidizing gases or chemical agents to develop and enhance its pore structure [36]. The increasing demand for activated carbon in pollution control applications, particularly in wastewater treatment, has resulted in higher production costs. This increase is mainly attributable to the dependence on non-renewable, costly, and regionally limited precursors, such as coal and petroleum pitch. As a result, there is a growing focus on discovering low-cost, renewable alternatives. Among these alternatives, activated carbon produced from agricultural residues has emerged as a promising option for environmental applications [37,38].

In this context, agricultural waste has attracted considerable attention as a sustainable resource for activated carbon production. These materials, particularly lignocellulosic biomass, are abundant, inexpensive, and rich in carbon content [39]. Corn, as a major crop consumed globally in various forms, generates significant amounts of agricultural residues, which are often underutilized. Converting these residues into value-added products, such as activated carbon, can enhance the sustainability and economic value of corn production [40]. This paper aims to comprehensively review the current state of research on heavy metal adsorption using activated carbon derived from corn waste biomass, assessing its potential as an efficient adsorbent. Based on the literature reviewed and the available studies on biomass-derived activated carbons, this review places particular emphasis on corn residues (such as cobs, husks, leaves, silk, and tassel) as promising precursors for carbon material synthesis. The present paper deals exclusively with activated carbon

materials synthesized from specific corn residues (cobs, husks, leaves, silk, and tassel) and provides a comprehensive critical discussion of their preparation routes, activation strategies, structural and surface characteristics, and adsorptive mechanisms toward heavy metal ions. By narrowing the scope and deepening the analysis, this review delivers a more detailed understanding of structure–property–performance relationships in corn-residue-based activated carbon materials, highlighting their unique potential and future prospects in heavy metal removal. The primary objectives of this review are to evaluate the feasibility of using corn agricultural residues as sustainable and low-cost precursors for activated carbon production, provide a detailed overview of preparation methods including carbonization and chemical/physical activation techniques applied to corn-derived biomass, analyze the characterization methods and textural properties of the produced activated carbon, compare the adsorption performance of corn waste-derived activated carbon in the removal of various heavy metal ions from aqueous solutions, and elucidate the underlying mechanisms of heavy metal removal by corn-based activated carbon. Figure 1 illustrates the overall workflow of this study, including pre-treatment of biomass, carbonization and activation, structural and surface properties, and adsorption of heavy metals.

Table 1. Permissible limits of heavy metals in drinking water according to WHO standards, their common sources, and related health effects.

Metal	Permissible Limits in Drinking Water [10]	Sources	Related Health Problems	Reference
As	10 g/L	naturally occurring in groundwater, mining	Skin, kidney, and bladder cancer, nausea, diarrhea, and muscle cramps	[9,11]
Cd	0.003 mg/L	electroplating, alloys, photographic development, ceramic, naturally occurring	vomiting, diarrhea, (acute) asthma, and tubular dysfunction (chronic inhalation)	[12,13]
Cr	0.05 mg/L (VI)	dyes and pigment manufacturing, wood preserving, electroplating	lung cancer, dermatitis, mutagenic	[14,15]
Cu	2 mg/L	urban and industrial wastewater	stomach and intestine problems, neurotoxicity, jaundice, and liver toxicity	[7,16]
Hg	1 µg/L	coalfired power plants, cement plants, and steel plants	adverse effects on the digestive tract, kidneys, capillaries, and nervous system	[17]
Fe	0.3 mg/L *	coatings, car, aeronautics, and steel industries	/	[18,19]
Mn	0.08 mg/L	naturally occurring, mining	neurological effects	[19]
Ni	bioavailable 4 µg/L (EU)	naturally occurring, electroplating, alloys, mining, waste incineration	skin irritation, dermatitis (dermal contact), nausea, vomiting, and diarrhea (ingestion), liver damage, and heart failure	[12,20]
Pb	0.01 mg/L	tanneries, electronics, electroplating, and petrochemical industries	nervous system disorders, kidney failure, cancer, and cardiovascular disease	[16,21]
Zn	3 mg/L	zinc water tanks, industrial wastewater	loss of appetite, decreased sense of taste and smell, slow wound healing, and skin sores	[12,16]
U	30 µg/L	radioactive waste	Kidney, bone, lung damage	[10,22]

* The limit for iron was based on aesthetic criteria and not human health.

Table 2. Advantages and Disadvantages of process methods for removing metal ions from water.

Process Methods for Removing Metal Ions from Water	Advantages	Disadvantages	Reference
Chemical precipitation	-Treatment of water with high metal ion content. -Could be performed at ambient temperature -Simple operation, -Low costs	-Requires a high amount of precipitating agent -Does not remove complex metals -Generation of a large quantity of sludge, -The need to add chemical reagents to adjust the pH value -Corrosive effect on equipment when using strong alkaline precipitators	[23–25]
Ion exchange	-For the wastewater treatment with low metal ion content. -Reusing resin after regeneration -Easy to automate	-Expensive resin, -Required wash-out solvent for impregnated resins -Slow operation rate	[24,26]
Electrochemical treatment	-Selective removal of metal ions -No additional reagents are required -No generation of sludge -The coagulant is formed in situ	-High energy costs -Consumption, degradation, and passivation of electrodes	[25,27–29]
Membrane filtration	-The removal of trace concentrations of metal ions -High degree of metal ion removal -Does not require chemical reagents -Ensure good water quality	-The cost of the technology and the possibility of membrane fouling limit their large-scale use -Loss of efficiency during multiple processes	[25,30,31]
Adsorption	-Simple process -Wide range of applications -Large specific surface area and porosity -Susceptible to regeneration -Low costs	-Low selectivity -Decrease in adsorptive capacity following multiple steps -Adsorptive power decreases at a high concentration of pollutants	[25,32–35]

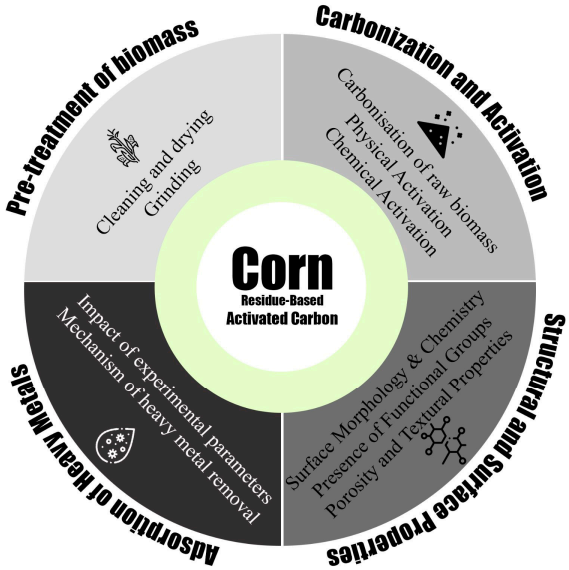


Figure 1. Schematic overview of the pre-treatment of biomass, carbonization and activation, structural and surface properties, and adsorption of heavy metals from aqueous solutions.

In this study, a total of 86 references published between 1984 and 2025 were used, with particular emphasis placed on literature from the past decade. The recent studies constitute the majority of the references and were employed to analyze current trends in the application of activated carbon for the removal of heavy metals from aqueous

solutions, whereas older publications were utilized to establish the fundamental theoretical framework and to trace the historical development of this research field. This approach provides a comprehensive overview of the evolution of studies in this area, from early experimental investigations to modern methods of synthesis and surface modification of activated carbon. The distribution of the utilized references by publication year is presented in Figure 2.

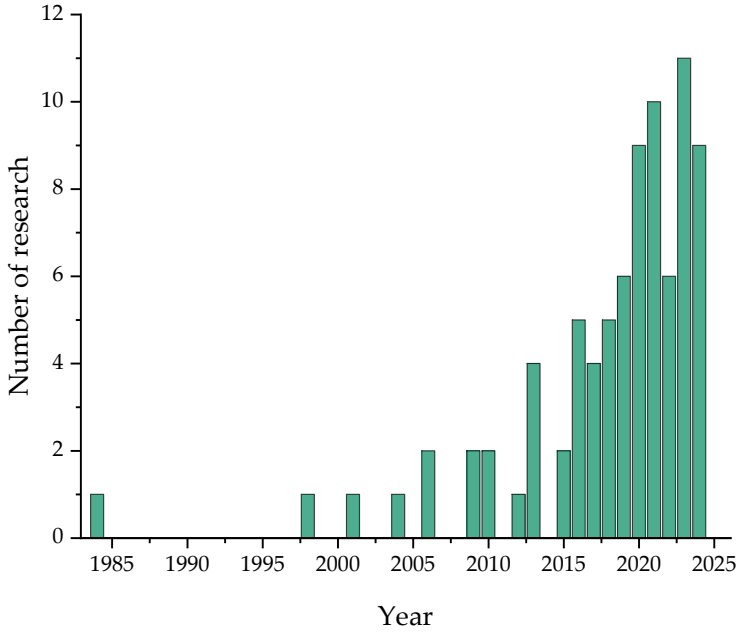


Figure 2. Distribution of research papers by year used in this study.

2. Corn Waste Biomass as a Raw Material for Activated Carbon Production

Corn (*Zea mays* L.) is one of the most widely cultivated cereal crops across temperate and tropical regions, primarily due to its versatile use in food, feed, fuel, and industry. Its cultivation generates a significant amount of agricultural residue, accounting for nearly half of the plant's dry mass, which is often burnt in open fields, causing environmental and health concerns. However, they have considerable potential for sustainable utilization, including their use as livestock feed, soil amendments, construction materials, bioenergy sources, biosorbents, or as precursors for activated carbon production [41,42]. Corn residues are rich in lignocellulosic components, primarily cellulose (37–40%), hemicellulose (21–25%), and lignin (18–20%), which make them particularly suitable for producing porous carbon materials with high specific surface area and excellent adsorption capacity [43]. An increasing number of studies have focused on the use of corn waste biomass for the preparation of activated carbon materials. This section summarizes significant research on utilizing different corn residues for this purpose. Among the various parts of the corn plant, corncobs have received the most attention in the literature due to their favorable chemical composition, centralized accumulation during processing (approximately 18 kg per 100 kg of grain), and low nutritional value, which minimizes competition with livestock feed [44–46]. In contrast, other corn residues, such as straw, husk, tassel, silk, and leaves, are more generally distributed across fields after harvesting and exhibit higher moisture content, which complicates their collection, drying, and further processing for industrial applications. Numerous studies have applied various chemical activation strategies to convert corncobs into porous carbon materials with excellent adsorption properties. For example, Christica et al. produced activated carbon by chemical activation with 5–15%

hydrogen peroxide, followed by carbonization at 450 °C, obtaining a material effective for heavy metal adsorption [40]. In another study, Liu et al. pretreated corncobs with 10% sulfuric acid at 170 °C, then mixed the intermediate product with KOH and applied chemical activation under controlled temperature conditions in an argon atmosphere. The resulting activated carbon reached a specific surface area value of 1054.2 m^2/g, demonstrating the efficiency of this approach [17]. In a similar approach, Liu et al. used corn cobs as a precursor for the production of activated carbon, which was first carbonized at 500 °C for 1 h under a nitrogen atmosphere and then mixed with KOH and activated through a two-step heating process. Finally, the KOH-modified carbon was further functionalized by soaking in a $KMnO_4$ solution to obtain $KMnO_4$-modified corn cob activated carbon [47].

While corncobs dominate literature, other parts of the corn plant have also shown potential. Corn stalks, for instance, have been successfully converted into activated carbon using activation agents such as KOH, $ZnCl_2$, and K_2CO_3, as demonstrated by Zhao et al. and Li et al. [48,49]. The resulting material demonstrated effective performance in Cr(VI) adsorption. Corn husks have been used in the production of amine-functionalized carbon materials for heavy metal removal, as reported by Ismail et al. Their multi-step chemical modification process involved epichlorohydrin, N,N-dimethylformamide, ethylenediamine, trimethylamine, and pyridine under controlled temperature conditions. The final functionalized product showed high efficiency in removing heavy metals from battery recycling wastewater [50].

Corn cob and stalk have been the most extensively studied as precursors for activated carbon production due to their favorable composition, abundance, and ease of processing. Husks have seen more limited application, while tassels and silk remain largely underexplored among corn residues.

For example, Olorundare et al. applied both physical (CO_2) and chemical (H_3PO_4) activation to corn tassels, obtaining materials with promising Pb(II) adsorption capacity [51]. These studies emphasize the potential of underutilized residues for valorization and environmental applications.

Overall, while cobs and stalks continue to dominate as feedstocks for activated carbon, husks and tassels and silk offer promising alternatives that require further investigation. Having established the suitability of various corn residues as precursors, the following section reviews preparation methods for activated carbon production from these materials.

3. Method of Production and Activation of Activated Carbon

3.1. Pre-Treatment of Biomass

Corn residues are initially collected and subjected to a cleaning process to remove impurities. The biomass is subsequently rinsed with distilled water to remove surface contaminants and residual soluble substances. The material is manually cut into smaller pieces, ground into a uniform powder, and sieved to isolate specific particle sizes, typically ranging from 0.09 to 8 mm, which are appropriate for subsequent synthesis. The prepared biomass is then subjected to carbonization and activation processes, depending on the desired properties of the final adsorbent.

3.2. Carbonization and Activation Methods

Activated carbon can be synthesized either directly from the raw biomass or via a two-step method involving carbonization followed by activation. In the second approach, the biomass is first carbonized, which is a thermal decomposition process carried out at elevated temperatures, typically below 700 °C, in the absence of oxygen. Carbonization removes volatile components and produces a carbon-rich residue known as char, carbonized material, or biochar, while altering the chemical and structural properties of the biomass to

prepare it for activation. The activation step is then applied to further develop the porosity and internal structure of the carbonized material, forming fine pores (predominantly mesopores and micropores) and increasing the surface area critical for adsorption processes [52]. Both physical and chemical activation methods have been employed depending on the specific application and desired porosity. Physical activation typically uses steam or CO_2, while chemical activation commonly employs phosphoric acid, potassium hydroxide, zinc chloride, or nitric acid, which promote pore formation and surface functionalization. Numerous studies have systematically investigated the effects of activating agents, synthesis methods, and processing parameters on activated carbon derived from corn biomass.

For example, Zhao et al. synthesized activated carbon from corn stalk powder using chemical activation with varying KOH concentrations (2–5%). The precursor was refluxed at 80 °C for 4 h, followed by filtration, washing, and drying at 100 °C overnight. Thermal activation was subsequently carried out at 600 °C for 1.5 h under a nitrogen flow rate of 100 mL/min. The resulting material exhibited excellent adsorption capacity for Cr(VI), with a maximum uptake of 89.5 mg/g [48]. In a similar effort to utilize alternative corn residues, Olorundare et al. employed milled maize-tassel powder activated with H_3PO_4 at different precursor-to-acid ratios (1:1–1:4). After impregnation and drying at 110 °C for 24 h, the samples were carbonized at 500 °C under nitrogen. Surface areas of activated carbons ranged from 623 to 1262 m^2/g, indicating well-developed porosity suitable for heavy metal removal [51]. To further enhance the porosity and surface structure, Latiff et al. applied a physicochemical activation approach using corncob (CC) as the biomass precursor. Although the particle size was not specified, the activation involved impregnation with potassium hydroxide followed by carbon dioxide gasification. The carbonization process was carried out in a vertical tubular reactor under a nitrogen flow of 150 cm^3/min, with a heating rate of 10 °C/min, up to a final temperature of 700 °C, maintained for 2 h. The activation process was optimized at a temperature of 797 °C, with an activation time of 3 h, and a KOH impregnation ratio (IR) of 3.5. This treatment resulted in the formation of activated carbon with enhanced structural properties suitable for further adsorption studies [53]. As can be seen in Table 3, several researchers have synthesized activated carbon from corncob waste through a two-step activation process, subsequently applying surface functionalization to improve adsorption efficiency. Liu et al. carbonized dried corncob at 500 °C in a nitrogen atmosphere, resulting in the formation of corncob carbon (CCC). In the second step, chemical activation involved impregnating CCC with potassium hydroxide under different activation temperatures, durations, and KOH-to-carbon mass ratios. The material underwent chemical activation with KOH under different conditions, including variations in temperature, duration time, and KOH-to-carbon ratio, utilizing a stepwise heating approach to reach the desired temperature. Following thorough washing to eliminate residual chemicals, the corn cob activated carbon material (CCAC) was subjected to drying at 105 °C. To enhance surface chemistry, CCAC was functionalized with $KMnO_4$, resulting in $KMnO_4$-modified corn cob activated carbon (CKAC) that exhibits increased oxygen-containing groups and improved contaminant removal efficiency [47]. A comparative overview of the synthesis parameters, activating agents, and functionalization methods used in these studies is provided in Table 3. This summary highlights the diversity of approaches used to tailor the structural and chemical properties of corn-based activated carbons and provides appropriate references for each approach, allowing for easier cross-referencing and comparison based on the type of activation process, temperature, and additional agents. In combination with the following chapters, this table clearly demonstrates how thermal and chemical treatments modify the structure and surface chemistry of corn waste-derived activated carbons and provides an overview of the methods used to produce corn waste-derived activated carbon materials.

3.3. Functionalization and Modification of Activated Carbon

Surface functionalization and modification refer to a process that aims to change the chemical characteristics of a material's surface to tailor its properties to particular applications [54]. Research has focused on enhancing and diversifying the surface properties of activated carbon through various treatment techniques to improve its effectiveness in removing specific contaminants from wastewater [55]. Activated carbon derived from corn waste has been modified using different agents, including $KMnO_4$, $FeSO_4 \cdot 7H_2O$, Ag nanoparticles (Ag NPs) and SiO_2 nanoparticles (SiO_2 NPs), and $FeCl_3$. Nethaji et al. modified activated carbon prepared from corn cob biomass, using the solution of ferrous sulfate and 10% sodium hydroxide solution to precipitate hydrated iron oxides. After stirring and heating the suspension at 100 °C for 1 h, they obtained a magnetized activated carbon material derived from corn cob (MCCAC). Characterization by SEM and TEM revealed a uniform distribution of magnetite nanoparticles (≈50 nm) on the corn cob activated carbon surface, with shapes ranging from cubic to spheroidal, indicating successful modification of activated carbon. BET analysis showed a surface area of 143 m^2/g and a pore volume of 0.212 cm^3/g, while unmagnetized carbon exhibited higher surface area (282 m^2/g) but lower pore volume (0.158 cm^3/g) The material was effectively used for the removal of Cr(VI) from aqueous solutions with a maximum monolayer adsorption capacity of 57.37 mg/g [14]. Nyirenda et al. synthesized an activated carbon-supported silver-silica nanocomposite (AC-Ag-SiO_2) using activated carbon derived from maize cobs. The composite was prepared by mixing activated carbon with silica nanoparticles and a colloidal silver solution. The mixture was stirred at 343 K followed by gel formation, dried at 353 K overnight, and calcined at 573 K for 2 h. FTIR analysis confirmed the functionalization, showing characteristic bands at 444, 803, 1066, 1396, 1556, and 3010 cm^{-1} corresponding to Si-O-Si stretching and bending, stretching vibrations of siloxane, C–H deformation, C=C stretching vibrations and O-H stretching vibrations, which confirms successful functionalization of activated carbon material from maize cobs [16]. Vaddi Dhilleswara Rao et al. synthesized a magnetic nanocomposite based on maize shell activated carbon (Fe_3O_4-MSAC). Fe_3O_4-MSAC was prepared by mixing maize shell activated carbon (MSAC) with aqueous dispersion of Fe_3O_4 nanoparticles. The mixture was stirred at 200 rpm for 1 h and then heated at 550 °C for 3 h. The resulting material was dried at 110 °C for 12 h. In this study, the authors did not provide FTIR or SEM analyses comparing the activated carbon material before and after functionalization. Instead, they only presented the FTIR and SEM results of the Fe_3O_4-MSAC composite before and after Cd adsorption. The FTIR spectrum of Fe_3O_4-MSAC shows a characteristic Fe–O stretching vibration band in the 400–600 cm^{-1} region, which may indicate successful functionalization of the activated carbon with iron oxide nanoparticles. The obtained Fe_3O_4-MSAC nanocomposite exhibited the presence of numerous small particles on the surface by SEM analysis, which suggests that the material has a high surface area, and enhanced adsorption performance due to the synergistic effect between Fe_3O_4 and the porous carbon matrix. XRD analysis revealed that the combination of crystalline and amorphous phases of materials provides abundant active sites for Cd(II) adsorption and leads to improved adsorption efficiency of the Fe_3O_4-MSAC composite [56]. Further functionalization of activated carbon materials is strongly encouraged, as it can significantly enhance their surface properties, create additional active sites, and improve their overall adsorption performance for targeted contaminants. The types of agents used for functionalization and the parameters of the functionalization and modification process are shown in Table 3.

Table 3. Preparation and Functionalization Parameters of Activated Carbons from Corn Waste Materials.

Biomass (Part of Corn)	Biomass Particle Size	Type of Activation, Activation Agents	Carbonization Parameters (T, Duration, Atmosphere)	Activation Parameters (T, Duration, Atmosphere, Mass Ratio)	Functionalization, Agents, Soaking Time	Reference
Maize tassel	45–212 µm	Physical, CO_2	300–700 °C, 1 h, 10 °C/min, N_2	300–700 °C,	/	[51]
Maize tassel	45–212 µm	Chemical, H_3PO_4 (85%)	/	500 °C, /, N_2, 1:1; 1:2; 1:3; 1:4	/	[51]
Corn cobs	≤180 µm	Chemical, KOH	500 °C, 1 h, 10 °C/min, N_2	500–900 °C, N_2, 0.5–2.5 h, 1:1–1:5; (statistical approach)	$KMnO_4$, 0.02–0.18 mol/L, 12 h	[47]
Corn stalk	0.5–1.0 mm	Chemical, KOH (2–5%)	600 °C, 1.5 h, /, N_2	80 °C, 4 h, reflux,—(2.0 g biomass/100 mL KOH sol.)	/	[48]
Corn husks	0.5–3.0 mm	Chemical, H_3PO_4 (ACP) Chemical, H_3PO_4 + $ZnCl_2$ (ACP-Zn) Chemical, H_3PO_4 + $ZnCl_2$ + $FeCl_3 \cdot 6H_2O$ (ACP-Zn-Fe)	700 °C, 2 h (heat rate: 500 °C in 1 h), N_2	Soaked in 50% H_3PO_4, dried at 80 °C (ACP), ACP + $ZnCl_2$ (sample/salt = 5:1), dried at 80 °C (ACP-Zn) ACP-Zn + $FeCl_3 \cdot 6H_2O$ treatment, dried at 80 °C (ACP-Zn-Fe)	/	[57]
Corn husk	/	Chemical, H_3PO_4	300 °C for 2 h, 500 °C for 1 h, 5 °C/min, N_2	Impregnation ratio 1:1 (*w*:*v*) H_3PO_4, 60 °C for 12 h, in stainless steel reactor	/	[58]
Corn cobs	/	Chemical, H_3PO_4	500 °C, 2 h	Impregnation ratios: 0.25, 0.5, 1, 1.5, 2 (*w*:*w*) stirring for 24 h; drying at 80 °C for 24 h	/	[21]
Corn cobs	/	Chemical, H_3PO_4	500 °C, 1 h, muffle furnace atmosphere 10 K/min	H_3PO_4 (*m*:*v* = 5:3), 113 °C, 16 h	/	[59]
Corn cobs	/	Chemical, H_2SO_4 pretreatment + KOH activation	400 °C, 30 min, 800 °C, 1 h; 10 °C/min; under Ar gas	10% H_2SO_4, 170 °C for 48 h, mixed with KOH (1:2 mass ratio)	/	[17]
Corn cobs	4–8 mm	Chemical, H_3BO_3	700 °C, 1 h, 5 °C/min, N_2	60 g CCs + 60 g H_3BO_3 in 700 mL H_2O, 70 °C for 6 h	/	[60]
Corn straw	/	Chemical, KOH	450 (30 min), 650 (30 min), 800 °C (60 min), 5 °C/min, N_2	KOH-to-biomass mass ratio 1:1	/	[15]
Corn cob	0.7–0.9 mm	Chemical, H_3PO_4, H_3BO_3	500 °C, 1 h	Pre-carbonized CC + activating agents, then HCl (37%) at 120 °C, 45 min	/	[12]
Corn cobs	≈150 µm	Chemical, H_3PO_4 + H_3BO_3	400, 450, 500 °C (varied), 1 h, muffle furnace	Immersed at 120 °C for 15, 30, or 45 min in acid mixture	/	[61]
Corn straw	≈150 µm	Chemical, H_3PO_4 + H_3BO_3	500 °C, 1 h, muffle furnace	Immersed at 120 °C for 45 min in acid mixture	/	[61]
Maize cobs	300 µm	Chemical, NaOH (1.0 M)	240 °C, 5 min	24 h, 300 g maize cobs: 1000 cm^3 NaOH	/	[20]
Maize plant biomass (tassels, cobs, stalks)	/	Chemical, H_3PO_4	500 °C, N_2	800 °C, N_2, H_3PO_4	/	[11]
Corncob (CC)	1–2 mm	Physicochemical, KOH + CO_2	700 °C, 2 h, N_2 atmosphere, 10 °C/min	797 °C, 3 h, CO_2 atmosphere, impregnation ratio = 3.5	/	[53]

Table 3. *Cont.*

Biomass (Part of Corn)	Biomass Particle Size	Type of Activation, Activation Agents	Carbonization Parameters (T, Duration, Atmosphere)	Activation Parameters (T, Duration, Atmosphere, Mass Ratio)	Functionalization, Agents, Soaking Time	Reference
Corncob	/	Physical, CO_2	500 °C, 2 h, air (muffle furnace), 20 °C/min	700 °C, 1.5 h, CO_2, pre-N_2 atmosphere, 20 °C/min	$FeSO_4 \cdot 7H_2O$ + NaOH (precipitation of Fe oxides), 100 °C, 1 h	[14]
Corncob	75–100 µm	Chemical, H_3PO_4 (85%)	500 °C, 2 h	Room temp, 12 h, solid–liquid ratio 1:5 (g/mL)	/	[18]
Corncob	75–100 µm	Chemical, $AlCl_3$	500 °C, 2 h	$AlCl_3$ (0.01 mol/L), 80 °C, 10 h	/	[18]
Corncob	/	Chemical, KOH	600 °C, 2 h, N_2 (100 cm^3/min), 5 °C/min	KOH:CCW = 4:1 (impregnated overnight), 600 °C, 2 h, N_2, 5 °C/min	/	[7]
Corncob	/	Chemical, HNO_3	600 °C, 2 h, N_2 (100 cm^3/min), 5 °C/min	65% HNO_3, 24 h soaking,	/	[7]
Corn straw	<1 mm	Chemical, H_3PO_4 (85%)	600 °C, 1.5 h, N_2	Impregnation in 85% H_3PO_4 for 24 h, 600 °C, 1.5 h, N_2	/	[9]
Corn straw	<1 mm	Chemical, H_3PO_4 (85%)	600 °C, 1.5 h, N_2	Impregnation in 85% H_3PO_4 for 24 h, 600 °C, 1.5 h, N_2	Post-treatment with $FeCl_3 \cdot 6H_2O$: 5 g AC in 500 mL $FeCl_3$ solution (40 g/500 mL) for 24 h, dried 12 h at 105 °C	[9]
Maize shells	/	Chemical, H_2SO_4	400 °C, 3 h, muffle furnace (air)	Impregnation ratio 1:1.8 (biomass: H_2SO_4)		[56]
Maize shells	/	Chemical, H_2SO_4	400 °C, 3 h	Impregnation ratio 1:1.8 (biomass: H_2SO_4), 105 °C drying	Fe_3O_4 nanoparticles (20 wt%), soaking for 1 h at 200 rpm, heating at 550 °C, 3 h	[56]
Corn husk	/	Chemical, H_3PO_4	400 °C, 30 min, muffle furnace (sealed ceramic container)	Impregnation ratio 1:2 (corn husk: H_3PO_4), 24 h	1.0 M citric acid (4 g CC to 25 mL) for 30 min, dried overnight at 50 °C	[62]
Maize cob	≤0.09 mm	Chemical, H_3PO_4 (75%)	500 °C, 20 min	Weight ratio H_3PO_4: char = 0.1, 60 °C for 24 h	/	[63]
Maize cob	2 mm	Chemical, 50% H_2SO_4 (AC-MC)	400 °C, 3 h, 10 °C/min, air atmosphere	Soaking ratio H_2SO_4:precursor = 2:1 (86 mL/60 g)	/	[16]
Maize cob	2 mm	Chemical, 50% H_2SO_4	400 °C, 3 h, 10 °C/min, air atmosphere	Soaking ratio H_2SO_4:precursor = 2:1 (86 mL/60 g)	Combined with Ag NPs and SiO_2 NPs in colloidal form, heated at 70 °C, dried at 80 °C, calcined at 300 °C for 2 h (AC-Ag-SiO_2 nanocomposite)	[16]
Corn husk	250 µm	Chemical, 2% HNO_3 (v/v) (CHAC)	300 °C, 2 h 20 °C/min, under N_2	30 g corn husk + 200 mL HNO_3, stirred 2 h		[50]

Table 3. *Cont.*

Biomass (Part of Corn)	Biomass Particle Size	Type of Activation, Activation Agents	Carbonization Parameters (T, Duration, Atmosphere)	Activation Parameters (T, Duration, Atmosphere, Mass Ratio)	Functionalization, Agents, Soaking Time	Reference
Corn husk	250 μm	Chemical, 2% HNO_3 (*v*/*v*)	300 °C, 2 h, 20 °C/min, N_2	30 g corn husk + 200 mL HNO_3, stirred 2 h	20 mL epichlorohydrin + 25 mL DMF + 11 mL ethylenediamine (80 °C, 1 h) + 25 mL trimethylamine (1 h) + 20 mL pyridine + 20 g CHAC (90 °C, 2 h), dried at 75 °C for 6 h (AF-CHAC)	[50]
Corn cob	≈355 nm	Chemical, KOH	700 °C, 2 h, 5 °C/min, N_2	KOH (1:0.3 wt)	/	[22]
Corn cob	≈355 nm	Chemical, KOH	700 °C, 2 h, 5 °C/min, N_2	CC:KOH:urea = 1:0.3:0.3	/	[22]
Corn cob	/	Chemical, KOH	480 °C, 1 h, N_2	85 wt% H_3PO_4: corn cob 40:60, 45 °C 24 h, KOH:char, (3:1 wt), 790 °C, 1 h, N_2	/	[64]

4. Structural and Surface Properties of Corn Waste-Based Activated Carbon

The characterization of activated carbon materials provides the necessary basis for the design and optimization of novel adsorbents, supports the selection of appropriate materials for specific applications, and facilitates the implementation of adsorption technologies at larger scales. A wide range of analytical techniques are available to examine the chemical structure, surface functionalities, and textural properties of carbon materials. Among the most frequently employed methods are Scanning Electron Microscopy (SEM), Fourier-Transform Infrared Spectroscopy (FTIR), X-ray Photoelectron Spectroscopy (XPS), Energy-Dispersive X-ray Spectroscopy (EDS), and X-ray Diffraction (XRD) [65]. Since each technique offers only partial insight, a multimodal characterization approach is recommended to achieve a more comprehensive understanding of surface chemistry and structural features, supported by the careful interpretation of complementary datasets [66]. This section examines in detail the adsorptive performance and properties of activated carbon materials obtained from different components of corn waste, emphasizing their physicochemical properties relevant for the extraction of heavy metals from aqueous solutions.

4.1. Surface Morphology and Surface Chemistry

Scanning Electron Microscopy (SEM) is widely utilized to observe morphological transformations occurring during the thermal and chemical processes involved in converting raw biomass into activated carbon. This technique offers valuable insights into the surface texture and structural evolution of the material. Additionally, SEM can be used to detect morphological alterations that arise as a result of adsorbate accumulation on the adsorbent surface, thereby providing visual evidence of adsorption phenomena [67]. Bozbeyoglu et al. examined the surface morphology of corn cob-based materials before and after chemical activation using SEM. The SEM image of the raw corn cobs (CCs) revealed a relatively dense and compact surface without visible porosity, although some surface irregularities such as roughness, indentations, and protrusions were observed. After chemical activation at 700 °C in a nitrogen atmosphere with boric acid as the activating agent, the morphology of the activated carbon was subjected to considerable changes. Numerous fractures, voids, surface channels, and cavities were formed due to thermal dehydration and structural reorganization induced by the activating agent. These morphological features indicate the development of a porous structure, which is essential for adsorption applications. The resulting enhancement in surface area, combined with the formation of new pores and functional groups, contributed to the improved adsorption performance of the material [60]. Similarly, Zhao et al. examined the morphological evolution of corn stalk-derived activated carbon using SEM before and after KOH treatment. The untreated corn stalks exhibited relatively smooth surfaces without noticeable porosity. In contrast, the sample activated with 3% KOH (AC-KOH (3%)) showed increased surface roughness and the appearance of initial pore structures, suggesting partial removal of cellulosic components by alkali activation. With increasing KOH concentrations (AC-KOH (4%) and AC-KOH (5%)), more significant morphological changes were observed. The SEM images revealed abundant, increasingly uniform porous channels, with a marked increase in the number and smaller size of pores. These findings confirmed that pore formation was directly influenced by the KOH concentration and that the alkali impregnation step plays a key role in modifying the surface structure of the adsorbent. The development of both micropores and mesopores, particularly at higher KOH dosages, further highlights the effectiveness of KOH activation in enhancing the adsorption performance of the resulting material [48].

4.1.1. Presence of Functional Groups

FTIR spectroscopy is commonly used to identify surface functional groups on adsorbent materials, while XPS provides complementary information about surface elemental composition and chemical states, including the types of carbon-carbon and carbon-oxygen bonds, the presence of oxygen-containing functional groups, and the relative abundance of elements [68]. Combining these techniques offers a comprehensive understanding of surface functionalities, which is essential for elucidating adsorption mechanisms and improving adsorbent performance [65]. Numerous studies have employed FTIR and XPS analyses to characterize activated carbons derived from various corn biomass precursors, highlighting the importance of surface functional group identification for optimizing adsorption properties.

For instance, Silva et al. investigated activated carbon fibers produced from corn husks via phosphoric acid activation and subsequent pyrolysis, focusing on the removal of Pb^{2+} and Cu^{2+} ions from aqueous media. FTIR analysis of the precursor material revealed characteristic lignocellulosic bands including hydroxyl (O–H) groups at 3300 cm^{-1}, aliphatic C–H stretching vibrations at 2918 cm^{-1}, carbonyl (C=O) groups between 1600 and 1450 cm^{-1}, and ether (C–O) bonds in the range of 1300–1000 cm^{-1}. After thermal activation, these bands were significantly reduced or disappeared, indicating the degradation of lignocellulosic structures. In contrast, an increase in the intensity of the peak at 1572 cm^{-1}, attributed to C=O stretching vibrations in lactones, ketones, and esters, indicated the formation of acidic surface functionalities that enhance adsorption affinity. Complementary XPS analysis confirmed the chemical changes induced by activation. High-resolution spectra for C 1s, O 1s, N 1s, and P 2p were obtained and analyzed. The survey spectrum indicated that carbon and oxygen were the predominant surface elements, as evidenced by the intense C 1s and O 1s peaks, while N 1s and P 2p signals were of significantly lower intensity, reflecting their relatively minor surface abundance. Deconvolution of the C 1s spectrum revealed peaks at 284.45 eV and 284.76 eV, corresponding to C=C and C–C bonds, while the peak at 287.45 eV was attributed to C=O bonds. The O 1s spectrum displayed three peaks at 530.8 eV, 532.1 eV, and 533.8 eV, assigned to C=O, C–OH, and COOR groups, respectively. Furthermore, the P 2p spectrum displayed peaks at binding energies of 132.7 eV and 133.6 eV, which were assigned to P=O and P–O bonds, confirming the successful incorporation of phosphorus into the surface structure of the activated carbon fibers through H_3PO_4 activation [58]. Similarly, Tang et al. analyzed activated carbon derived from corn cobs using FTIR and XPS. The FTIR spectrum of raw corn cob exhibited characteristic bands at 2919 cm^{-1} (C–H stretching vibrations) and 1042 cm^{-1} (C–O stretching in cellulose), both of which disappeared after activation. The broad band around 3410 cm^{-1} corresponded to O–H stretching, whereas the spectrum of the activated carbon exhibited a marked band at 1064 cm^{-1}, attributed to C=O stretching, indicating enhanced carbonyl functionalities. Additional peaks at 2362 cm^{-1} and 883 cm^{-1} were assigned to the presence of CO_2 and Si–O–Si groups, respectively. High-resolution C 1s spectra were used to identify the chemical states of carbon on the surface of activated carbon. Deconvolution of the C 1s signal revealed four peaks assigned to C–C (284.8 eV), C–O/C–OH (286.0 eV), C=O (287.6 eV), and –COOH (289.7 eV) [69]. These studies collectively demonstrate that chemical activation not only modifies the porous structure of corn residue-derived carbons but also enriches their surface chemistry with oxygen-containing functional groups, which are essential for enhancing interactions with heavy metal ions and improving adsorption efficiency.

4.1.2. Porosity and Textural Properties

Surface area, pore diameter, and pore volume are critical textural parameters that strongly influence the adsorption performance of synthesized activated carbon materi-

als. These parameters are typically determined using nitrogen adsorption–desorption isotherms, analyzed through the Brunauer–Emmett–Teller (BET) and Langmuir models [70]. Cao et al. investigated the influence of process parameters on the development of the porous structure of activated carbon derived from corn cobs via KOH chemical activation with soap as a surfactant. Their study examined the effects of activation temperature, duration time, the KOH-to-carbonized material ratio, and activation technique. The experimental procedure involved carbonization at 450 °C for 4 h under a nitrogen atmosphere, followed by activation at 850 °C for 1.2 h using a KOH-to-carbon ratio of 4.0. Before activation, the carbonized material was immersed in a KOH and soap solution for 30 min. The resulting activated carbon exhibited a BET surface area of 2700 m^2/g, with a narrow pore size distribution dominated by micropores, which accounted for 78% of the total porosity [71]. Liu et al. studied the relationship between surface textural properties and the adsorption performance of corn cob-derived activated carbons. The carbonized sample (CC) obtained at 500 °C showed a BET surface area of 11.16 m^2/g and a total pore volume of 0.003 cm^3/g. After KOH activation, the CCAC sample displayed a significant increase in surface area (2797.75 m^2/g) and total pore volume (1.36 cm^3/g), resulting in enhanced mercury ion removal. Subsequent modification with potassium permanganate produced the CKAC sample, which exhibited reduced surface area (1212.93 m^2/g) and pore volume, likely resulting from pore blockage by deposited manganese oxides. Nitrogen adsorption–desorption isotherms for both CCAC and CKAC were classified as type I, indicating predominantly microporous structures. CKAC showed a slower increase in nitrogen uptake compared to CCAC, suggesting a lower micropore content [47]. A comprehensive overview of the key textural parameters (BET surface area and pore diameter) is provided in Table 4. The aforementioned analyses of surface morphology, functional group distribution, and porosity clearly illustrate how thermal and chemical treatments modify the structure and surface chemistry of corn waste-derived activated carbons. From our perspective, these structural and functional changes are directly relevant for metal adsorption: the formation of abundant micropores and mesopores increases the accessible surface area and diffusion pathways, while the introduction of oxygen and nitrogen-containing functional groups (–COOH, –OH, $–NH_2$) provides active sites for ion exchange, complexation, and electrostatic interactions with metal ions. Therefore, the combination of developed porosity and modified surface chemistry is critical for achieving high adsorption efficiency and selectivity toward heavy metals.

4.1.3. Determination of Surface Charge

The point of zero charge (pH_{pzc}) represents the pH at which the surface charge of the adsorbent is zero, i.e., the number of positively and negatively charged surface sites is equal. Understanding the pH_{pzc} is crucial for predicting the ionization of surface functional groups and their interactions with metal ions in solutions. When the solution pH exceeds the pH_{pzc}, the adsorbent surface becomes negatively charged, favoring adsorption of cations, whereas at pH values below the pH_{pzc}, the surface is positively charged, promoting anion adsorption [72]. Based on the data shown in Table 4, activated carbons derived from corn waste exhibit a wide range of pH_{pzc} values, typically from below 2 up to 7.5, reflecting variations in synthesis conditions, activation methods, and surface functionalization. In some studies, surface charge has been characterized not only through pH drift methods but also using zeta potential measurements and pH of slurry. Among the tested materials, the lowest pH_{pzc} value was recorded for CKAC, which was obtained by impregnating CCAC with potassium permanganate. The significant reduction in pH_{pzc} observed for CKAC and other modified samples indicates a high density of surface acidic groups. FTIR analysis confirmed that $KMnO_4$ treatment enhanced surface oxidation, introducing

a greater abundance of oxygen-containing functionalities and thereby increasing surface acidity [47]. In contrast, Nethaji et al. reported that magnetite-coated corn cob activated carbon (MCCAC) exhibited a predominantly basic surface characteristic, with a pH_{pzc} of 7.5. Boehm titration data supported this observation, revealing a higher concentration of basic (0.2592 meq/g) compared to acidic (0.066 meq/g) surface groups [14]. Zeta potential measurements provide complementary information on surface charge and acid-base behavior [73]. Hou et al. reported zeta potentials of 16.8 mV, −37.5 mV, and 23.75 mV for Oxide-CCW, CCW, and Cal-CCW, respectively, indicating that CCW possesses a negatively charged surface, whereas Oxide-CCW and Cal-CCW are positively charged under the measured conditions [7]. The obtained values are presented in Table 4, which summarizes the textural properties and surface charge characteristics of the synthesized activated carbons from corn waste. Comparing the activated carbon materials derived from corn residues, CCAC and other KOH-activated samples (such as a KM series activated carbons) exhibit the highest S_{BET} and dominant microporosity, indicating superior adsorption potential, whereas H_3PO_4-activated samples (2-20CCACp, ACP) show moderate surface areas with well-preserved oxygen functionalities, enhancing surface acidity and ion-binding capacity. Physically activated samples (PAC1-PAC5), with very low surface areas, display limited adsorption efficiency. Thus, these observations directly support the evaluation of material suitability for heavy metal removal, aligning with the objectives of this study.

Table 4. Textural Properties and Surface charge parameters of Synthesized Activated Carbons from corn waste.

Activated Carbon	S_{BET} (m^2/g)	Pore Diameter	pH_{pzc}, pH Slurry, Zeta Potential (mV)	Reference
Activated carbon/corn cob (KOH/soap activation)	2630	Micropores (78.3%): 0.2–2 nm Mesopores (14.3%): 2–53 nm Macropores (7.4%): 53–100 nm	/	[71]
Activated corn cobs	249	1.853 nm	/	[74]
AF-CHAC	442.70	/	6.8	[50]
CCA1 CCA2 CCA3 CCA4	712.16 776.23 623.26 1262.50	2.095 nm 3.209 nm 3.959 nm 4.881 nm	/	[51]
PAC1 PAC2 PAC3 PAC4 PAC5	5.82 4.21 6.46 13.04 75.60	5.320 nm 5.034 nm 5.969 nm 4.111 nm 1.924 nm	/	[51]
CCC CCAC CKAC	11.16 2797.75 1212.93	/ / /	2.03 3.49 pH_{pzc} less than 2	[47]
Activated carbon from corn cob	1054.2	2.41 nm	/	[17]
AC KOH (2% KOH) AC KOH (3% KOH) AC KOH (4% KOH) AC KOH (5% KOH)	498.0 566.1 565.8 565.3	3.87 nm 4.84 nm 4.63 nm 4.14 nm	/	[48]
ACF	1824	1–4 nm	3.85	[58]
Activated carbons from corn cob ($ZnCl_2$ and NH_4Cl)	924.9	1.17 nm	/	[69]
Porous carbon material prepared from corn straw-KOH activation agents	2131.181	0.5–1 nm (10 nm)	4.76	[15]
CCAC CSAC	840.2542 816.4197	<0.154 mm	/	[61]
MCCAC-Fe_3O_4	282	/	7.5	[14]

Table 4. *Cont.*

Activated Carbon	S_{BET} (m^2/g)	Pore Diameter	pH_{pzc}, pH Slurry, Zeta Potential (mV)	Reference
CAC-Al	146.64	2.747 nm	/	[18]
Cal-CCW	88	0.58 nm	16.8 mV	[7]
Base-CCW	296	0.46 nm	−37.5 mV	
Oxide-CCW	231	0.52 nm	23.75 mV	
Cal-Oxide-CCW (HNO_3)	8	0.56 nm		
CM-550	196	1.36 nm	7.5 (pH Slurry)	[75]
KM-33 (33% wt of KOH)	619	1.14 nm	8.4 (pH Slurry)	
KM-50 (33% wt of KOH)	1236	0.83 nm	8.9 (pH Slurry)	
KM-66 (33% wt of KOH)	1523	0.99 nm	9.3 (pH Slurry)	
KM-75 (33% wt of KOH)	1414	1.10 nm	9.9 (pH Slurry)	
AC	563.93	/	/	[9]
AF	217.87			
3-20CCACz, (3:1), 20% $ZnCl_2$	1270	2.10 nm	/	[76]
1-20CCACz (1:1), 20% $ZnCl_2$	616	1.87 nm		
3-40CCACz (3:1) 40% $ZnCl_2$	828	1.74 nm		
2-20CCACp (H_3PO_4)	553	2.28 nm		
3-20CCACs (H_2SO_4)	556	1.09 nm		
CS-AC	7.335	98.53 (average pore width, Å, 9.85 nm)	/	[77]
CS-HC-AC	331.233	24.36(average pore width, Å, 2.44 nm)		
CCs-AC	598.6	2.12 nm	4.98	[8]
ACP	474	1.95 nm	5.21	[57]
ACP-Zn (50% H_3PO_4/$ZnCl_2$)	227	3.84 nm	3.37	
ACP-Zn-Fe (50% H_3PO_4/$ZnCl_2$/$FeCl_3$)	186	5.86 nm	4.21	
Corn cob activated carbon (impregnation ratio 1:1 H_3PO_4)	S_L(m^2/g) 810 (Langmuir isotherm)	/	3.8	[21]
Corn cob activated carbon	/	/	3.0	[59]
CCAK7	915	1.15	/	[22]
CCAKN7	1395	0.95		

5. Adsorption Performance of Activated Carbon for Heavy Metal Removal

Adsorption studies of activated carbons produced from corn waste are typically performed in batch mode to evaluate the effects of key operational parameters. Factors such as solution pH, contact time, adsorbent dosage, and temperature strongly influence the adsorption efficiency of heavy metals, making their optimization essential for achieving maximum performance. Nevertheless, advanced statistical tools like response surface methodology–central composite design (RSM-CCD) offer a more efficient alternative. Manual optimization still dominates, although it is time-consuming, costly, requires numerous experiments, and may not adequately examine synergistic interactions among variables (e.g., pH and dose of adsorbent) [11]. To address this gap, statistical optimization is strongly recommended to efficiently optimize parameters and enhance adsorption performance for practical applications. It was noted that most of the research reviewed primarily focused on the removal of highly toxic and frequently present metal ions, including cadmium, arsenic, lead, nickel, zinc, copper, and mercury. Table 5 presents the key findings from reviewed studies, including adsorbent material (activated carbon), targeted metals, adsorption capacities (q_{max}), and key adsorption parameters (including pH, contact time, adsorbent dosage, and initial concentration).

5.1. Impact of pH

pH is a critical parameter in adsorption, influencing the ionization of functional groups and the speciation of metal ions in solutions. At low pH values, the surface of activated carbon becomes positively charged due to the high concentration of H^+ ions, which compete with metal cations for available adsorption sites, thereby reducing removal efficiency. As the pH increases, the surface charge shifts toward negative values, enhancing electrostatic attraction between the adsorbent and positively charged metal ions and thus improving adsorption. However, at excessively high pH values, metal hydroxides may begin to precipitate, limiting the effectiveness of adsorption [13]. A review of the literature on corn waste-derived activated carbons is typically conducted within a pH range of 2–8, although certain studies have explored a broader pH range, including highly alkaline conditions. Optimal pH values vary among metal ions; for example, Cr(VI) is typically best adsorbed at pH 2–4, while Pb(II) shows higher uptake near pH 4–8. These differences arise from variations in metal speciation, ion-surface interactions, and the surface chemistry of the adsorbent, which depends on its preparation conditions and activation method. Ismail et al. evaluated the adsorption of Pb(II), Cu(II), and Ni(II) using amine-functionalized corn husk activated carbon (AF-CHAC) at a pH range of 2–11. Removal efficiencies increased between pH 2 and 8: from 40.08% to 99.50% for Pb(II), 36.66% to 94.51% for Cu(II), and 32.45% to 90.04% for Ni(II). This trend was attributed to reduced H^+ ion competition and enhanced electrostatic attraction above the point of zero charge (pH_{pzc} = 6.8). Below this pH, protonation of surface groups caused repulsion and reduced metal uptake. At pH > 8, metal hydroxide precipitation decreased the adsorption efficiency [50]. Similarly, Bozbeyoğlu and Gündoğdu studied Cr(VI) adsorption on corn cob-derived activated carbon (CCs-AC) in a pH range of 2–8. The highest uptake occurred at pH 2, where the adsorbent surface was positively charged and favored electrostatic attraction with anionic species like $HCrO_4^-$. As pH increased, CrO_4^{2-} species dominated, and electrostatic repulsion led to reduced adsorption. Thus, pH 2 was identified as optimal for Cr(VI) removal. Therefore, the optimum pH value for Cr(VI) adsorption onto CCs-AC was determined to be 2 [60]. Liu et al. investigated the effect of pH on the adsorption of Hg(II) ions using CCAC and commercially available coconut shell carbon (C-CSC) adsorbents in a pH range of 3–11. Adsorption efficiency increased with increasing pH up to 7, reaching 95.3% for CCAC and 57.1% for C-CSC. Further increase in pH (from 7 to 11) resulted in a rapid decrease in Hg(II) removal, indicating unfavorable conditions for adsorption at higher pH values [17]. These studies collectively demonstrate that the effect of pH on adsorption is highly metal-specific and strongly correlated to the surface chemistry of the adsorbent. Appropriate control of pH conditions is therefore crucial for optimizing adsorption performance, particularly in real wastewater treatment applications.

5.2. Impact of Contact Time and Kinetic Modeling

Contact time is a critical parameter in adsorption studies, as it determines both the adsorption kinetics and the point of equilibrium [70]. In the context of contact time, the adsorption process is characterized by two distinct phases: (1) an initial rapid phase, quantitatively predominant, and (2) a subsequent slower phase that contributes minimally to the overall uptake. The first phase is characterized by a high adsorption rate due to the abundance of available active sites on the adsorbent surface. As these sites become progressively occupied, the process transitions into the slower phase, during which the adsorption rate decreases and gradually approaches equilibrium [78]. Literature on corn-based activated carbons confirms that contact time significantly influences adsorption kinetics and capacity. In most experiments, adsorption occurs rapidly in the initial stage and is followed by a slower phase as the system approaches equilibrium. The total equilibrium time varies

considerably depending on the type of metal ion and the physicochemical properties of the adsorbent, while the initial metal ion concentration may also influence the equilibrium time in certain systems. Reported equilibrium times range from 5 min to several hours. Prolonging the contact time beyond equilibrium generally has a negligible effect on further adsorption, confirming that maximum uptake is typically achieved within a well-defined period [22,79,80]. El-Bendary et al. investigated the effect of contact time on Fe(III) removal using CAC and its aluminum chloride-modified form (Al-CAC). A rapid uptake of Fe(III) occurred within the first minute, attributed to the abundance of available surface sites, followed by a slower phase (1–5 min) as a consequence of intraparticle diffusion, after which equilibrium was reached. Maximum removal efficiencies were 86.1% for CAC and 98.7% for Al-CAC, highlighting the enhancement achieved by aluminum modification. Prolonged contact time (beyond 30 min) led to partial desorption, likely due to weakened adsorbate–adsorbent interactions. Kinetic modeling revealed that the pseudo-second-order model provided the best fit to the experimental data, with a correlation coefficient (R^2) of 0.999 for both adsorbents at 25 °C. Furthermore, the calculated equilibrium adsorption capacities (q_e) were in close agreement with the experimental values, supporting the conclusion that chemisorption was the rate-limiting step [18]. Campos et al. studied Cu^{2+} and Ni^{2+} adsorption on corn cob activated carbon in both mono- and bicomponent systems. The contact time had a significant effect on the adsorption dynamics. In a monocomponent system, most uptake occurred within 50 min, with equilibrium reached at 240 min for Cu^{2+} and 100 min for Ni^{2+}. In the bicomponent system, the presence of both ions led to competitive interactions, extending the equilibrium time beyond 350 min. Initially, both ions were rapidly adsorbed due to the abundance of active sites. However, after 100 min, the amount of adsorbed Ni^{2+} began to decrease, while Cu^{2+} uptake continued to increase. This was attributed to the higher affinity of the adsorbent for Cu^{2+}, resulting in competitive desorption of Ni^{2+} ions from adsorption sites. The pseudo-second-order (PSO) model best described monocomponent kinetics ($R^2 \geq 0.618$), suggesting chemisorption governed by functional group interactions. In the bicomponent system, the parallel model (PM) better fits the data, especially for Ni^{2+}, which was more influenced by Cu^{2+} presence. Adsorption and desorption rate constants (k_a and k_d) were higher for Cu^{2+}, indicating stronger interaction kinetics [59]. Tang et al. investigated the adsorption of Cr(VI) using activated carbon derived from corn cobs, prepared by chemical activation with a $ZnCl_2/NH_4Cl$ mixture. Cr(VI) removal increased rapidly in the first 2 h, continued to increase more gradually until 4 h, and then showed no significant change, indicating that equilibrium was reached after 4 h. To evaluate the adsorption kinetics, pseudo-first-order (PFO) and pseudo-second-order models were employed. The PSO model provided a better fit ($R^2 = 0.998$), and its calculated equilibrium adsorption capacity ($q_e = 14.493$ mg/g) was closer to the experimental value (15.13 mg/g). These results suggest that the adsorption process followed a chemisorption mechanism [69]. Giraldo et al. investigated the adsorption kinetics of U(VI) using activated carbon samples derived from corncob (CCAKN7, CCAK7, and CC). Analysis of the correlation coefficients (R^2) for the different kinetic models indicated that the pseudo-second-order (PSO) model provided the best fit for all samples, suggesting that the adsorption process is primarily controlled by chemisorption. In addition to the pseudo-first-order, PSO, and Elovich models, the intraparticle diffusion model was also applied to gain insight into the uptake of U(VI) ions into the adsorbent pores. The analysis revealed that adsorption occurs in two stages: an initial surface diffusion followed by intraparticle diffusion. The presence of non-zero intercepts in the interparticle diffusion plots indicates that boundary layer effects contribute to the rate-limiting steps, meaning that intraparticle diffusion is not the only controlling factor. Overall, these results suggest that U(VI) adsorption on all three activated carbon samples is governed by a combination of chemical interactions and

diffusion processes within the pores, with the slower interparticle diffusion phase primarily determining the overall adsorption rate [22]. Table 5 shows the range of contact times reported in studies of activated carbon materials derived from corn waste.

5.3. Impact of the Dose of Adsorbent

Adsorbent dosage is a key parameter in optimizing adsorption processes, as it directly affects the number of available active sites and, consequently, the overall removal efficiency. Increasing the adsorbent mass generally enhances the total surface area and improves accessibility of binding sites. Nevertheless, beyond a certain threshold, adsorption performance may decline, likely due to particle aggregation, which reduces the effective surface area and limits adsorbate–adsorbent interactions [78]. A wide range of adsorbent dosages is typically examined to evaluate how the availability of active sites influences adsorption efficiency. Mayowa Adeoye Lala et al. investigated the effect of adsorbent mass on the removal efficiency of Ni(II) using maize cob-derived activated carbon (MCAC). Experiments were conducted at room temperature for 120 min, using a fixed initial Ni(II) concentration of 9.85 mg/L and an agitation speed of 120 rpm. The tested adsorbent amount ranged from 0.2 to 1.0 g. Removal efficiency increased progressively with adsorbent mass, reaching a maximum at 0.8 g. This was attributed to the increased surface area and greater number of available adsorption sites. A slight decrease was observed when the amount of activated carbon was further increased to 1.0 g, likely due to particle agglomeration and overlapping of active sites. Based on these results, 0.8 g of MCAC was identified as the optimal dosage for efficient Ni(II) removal [20]. Similarly, Tang et al. examined the influence of adsorbent dosage on Cr(VI) removal using activated carbon derived from corn cobs. Adsorption experiments were carried out at room temperature with 50 mL of Cr(VI) solution (initial concentration 10 mg/L) at pH 5.8. Adsorbent dosages ranging from 0.2 to 2.0 g/L were tested, with agitation at 180 rpm for 12 h. The results showed that the removal efficiency increased with increasing adsorbent dosage, which was attributed to the higher surface area and greater number of available adsorption sites. Complete removal (100%) of Cr(VI) was achieved at 0.7 g/L, whereas only 78.9% removal was obtained at 0.5 g/L. These findings highlight the strong dependence of Cr(VI) removal efficiency on the applied adsorbent dosage [69].

5.4. Impact of Initial Concentration

The initial concentration of metal ions is a key factor influencing adsorption efficiency, as it determines the availability of surface functional groups responsible for ion binding and alters the driving force for mass transfer between phases [81]. For instance, Nyirenda et al. evaluated several adsorption parameters of a silver–silica-modified activated carbon (AC-Ag-SiO_2) composite for the removal of Cu^{2+}, Pb^{2+}, Cd^{2+}, and Zn^{2+} ions, including the effect of initial metal ion concentration on removal efficiency. As the initial concentrations of these ions increased from 10 to 100 mg/L, removal efficiencies decreased from 94.46% to 72.53% for Cu^{2+}, 99.15% to 77.35% for Pb^{2+}, 90.30% to 68.57% for Cd^{2+}, and 97.49% to 74.97% for Zn^{2+}. This decline was attributed to the saturation of adsorption sites, which limited their ability to adsorb additional ions [16]. Similarly, El-Bendary et al. reported that increasing the initial concentration of Fe^{3+} ions from 5 to 40 mg/L using corn cob activated carbon (CAC) and its aluminum chloride-modified counterpart (Al-CAC) led to a decrease in removal efficiencies from 89.3% to 34.9% for CAC and from 99.1% to 66.7% for Al-CAC. The authors attributed this trend to the formation of larger iron ion aggregates or micelles at higher concentrations, which obstruct diffusion through the micropores of the adsorbents. In contrast, the adsorption capacity increased linearly within the same concentration range, from 39.3 to 334.9 mg/g for CAC and from 49.1 to 366.7 mg/g for

Al-CAC. This behavior was attributed to the enhanced concentration gradient and reduced mass transfer resistance, which collectively facilitated greater uptake of Fe^{3+} ions onto the adsorbent surface [18]. Further supporting these observations, Liu et al. examined Hg(II) adsorption on CCAC over initial concentrations ranging from 20 to 100 µg/L. Their results showed that adsorption rates increased as initial Hg(II) concentration rose from 20 to 40 µg/L, reflecting the increased driving force for mass transfer. However, removal efficiency decreased beyond 60 µg/L due to saturation of active adsorption sites. Comparisons with C-CSC revealed that CCAC exhibited superior adsorption capacity and less of a decrease in efficiency at higher concentrations, as a result of a greater abundance of oxygen-containing functional groups generated during KOH activation [17]. Table 5 compiles all the collected data regarding activated carbon capacities, targeted heavy metals, and adsorption conditions. Together with Table 4, these data provide a comprehensive overview of the preparation, functionalization, tested heavy metals, optimal conditions, and adsorption performance of activated carbons derived from corn waste.

From Table 5, it is evident that the highest adsorption capacity is 643.92 mg/g for copper using citric acid-functionalized corn husk activated carbon (CA-CHAC) [62]. Other notable values for adsorption capacities include 206.01 mg/L for lead with ACF [58], 500 mg/L for iron with CAC, 227.32 mg/L for mercury with CKAC [47] and 175.44 mg/L for chromium with carbon derived from corn straw [15]. These results clearly illustrate that KOH-activated and chemically or surface-functionalized carbons generally exhibit the highest adsorption capacities, whereas H_3PO_4-activated samples show moderate capacities due to their less developed porosity but well-preserved surface functionalities, highlighting the crucial role of both pore structure and surface chemistry in heavy metal removal.

Table 5. Overview of Adsorption Performance of Activated Carbons from Corn Waste for Heavy Metal Removal under Different Experimental Conditions.

Activated Carbon	Adsorbate	q_{max}	Adsorption Parameters (pH, Contact Time, Adsorption Dose, Initial Concentration-Ic)	Reference
Amine-functionalized corn husk activated carbon	Pb (II), Cu (II), Ni (II)	2.814 mg/g, 0.724 mg/g, 0.337 mg/g	pH 2–11 optimal value (o.v.) 8 1–7 g/L o.v. 4 g/L 0–120 min o.v. 60 min Ic/	[50]
CCA PAC1	Pb (II)	/	pH 0–7 o.v. 7 0–0.1 g o.v./ 0–400 min o.v./ Ic/	[51]
Activated carbon from corn cobs	Fe, Mn	/	pH 2–8 o.v. 4 0.1–2 g o.v. 1 g (Fe) 0.5 (Mn) 10–120 min o.v. 60 min (Fe) 30 min (Mn) Ic/	[19]
CCC CCAC CKAC-$KMnO_4$	Hg	175.88 mg/g 227.32 mg/g	pH 2–6 o.v. 4 (CCAC) 3 (CKAC) 0.20–1.00 g/L 0.40 g/L (CCAC) (CKAC) 15–1440 min. 120 min (CCAC) 60 min (CKAC) Ic 40–120 mg/L o.v. 100 mg/L (CCAC, CKAC)	[47]
CCAC	Hg	2.39 mg/g	pH 3–11 o.v. 7 10–80 mg/L o.v. 20 mg/L 0–120 min o.v. 120 min Ic 20–100 µg/L o.v. 60 µg/L	[17]
AC-KOH (4)	Cr (VI)	88.106 mg/g	pH 4.5 2.5 g/L 0–48 h o.v. 2 h Ic 50–300 mg/L	[48]

Table 5. *Cont.*

Activated Carbon	Adsorbate	q_{max}	Adsorption Parameters (pH, Contact Time, Adsorption Dose, Initial Concentration-Ic)	Reference
ACP-Zn (50% $H_3PO_4/ZnCl_2$) ACP-Zn-Fe (50% $H_3PO_4/ZnCl_2/FeCl_3$)	Cr (VI)	24.8 mg/g 30.3 mg/g	pH 2–8 o.v. 2–2.5 0.25 to 2.0 g/L o.v. 1 g/L 15–300 min o.v. 240 min Ic 5–30 mg/L o.v. 12 mg/L	[57]
ACF-H_3PO_4	Pb^{2+}, Cu^{2+}	206.01 mg/g (Pb^{2+}) 212.29 mg/g (Cu^{2+})	pH 2–5 o.v. 4–5 25 mg 0 to 360 min o.v. 100 min Ic 25 to 700 mg/L	[58]
Corn cob-based AC	Cr (VI)	34.48 mg/g (298 K)	pH 2–9 o.v 1–2 0.2 to 2.0 g/L o.v 0.7 g/L 0–7 h o.v. 4 h Ic m 8–20 mg/L	[69]
Corn cob activated carbon (H_3PO_4) 1:1	Pb^{2+}, Cu^{2+}	8 mg/g	pH 2–8 o.v. 5.3 (Pb^{2+}) 5.7 (Cu^{2+}) 0.07–0.2 g o.v. 0.1 g (Pb^{2+}) 0.2 g (Cu^{2+}) 5–120 min o.v. 60 min (Pb^{2+}), 90 min (Cu^{2+}) Ic 10–50 mg/L	[21]
Corn cob activated carbon (H_3PO_4)	Cu^{2+}, Ni^{2+}	0.39 mmol/g Cu^{2+} 0.28 mmol/g Ni^{2+}	pH 2–7 o.v 4 3–480 min 240 min Cu^{2+} 100 min Ni^{2+} Ic. 0.10 to 2.00 mmol/L	[59]
CCs-AC-H_3BO_3	Cr (VI)	123.7 mg/g	pH 2–8 o.v. 2 5 g/L 0–780 min o.v.4 h Ic 50–1000 mg/L	[60]
Carbon derived from corn straw	Cr (VI)	175.44 mg/g	pH 1–9 o.v. 3 1 g/L 0–600 min o.v. 480 min Ic 100–350 mg/L	[15]
GACC (H_3PO_4, H_3BO_3, HCl)	Cd^{2+}, Ni^{2+}, Zn^{2+}	0.21 mg/g, 0.19 mg/g, 0.28 mg/g	0.1–2 g o.v. 1 g 0–12 h o.v. 6 h Ic. 2–10 mg/L	[12]
CCAC, (H_3PO_4, H_3BO_3)	Cr (VI)	9.6246 mg/g	pH- 1–13 o.v. 7 0.5–2 g/L o.v. 1.0 g/L 5–60 min o.v. 60 min Ic 0.5–10 mg/L	[61]
MCAC	Ni (II)	/	pH/ 0.2–1 g. o.v. 0.8 g 15–150 min o.v. 120 min Ic o.v. 9.75 mg/L	[20]
Activated carbon produced from maize plant biomass	As (III)	/	pH 6 0.50–3.00 g/L o.v. 0.5 g/L 40.00–90.00 min o.v. 90 min Ic 10.00–30.00 mg/L o.v. 10 mg/L	[11]
MCCAC	Cr (VI)	120 µm 57.372 mg/g 600 µm 52.246 mg/g 1200 µm 54.94 mg/g	pH 2–11 o.v. 2 0.01 g/10 mL-0.1 g/10 mL o.v. 0.1 g/10 mL Ic. 100–1000 mg/L	[14]
CAC Al-CAC ($AlCl_3$)	Fe (III)	500 mg/g 250 mg/g	pH 4–10 o.v. 8 0.01–2 g/L o.v. 0.1 g/L 0–30 min o.v. 5 min Ic 5–40 mg/L	[18]
MLAC	Pb (II)	3.7136 mg/g	pH 2–8 o.v. 4 0.5 g 0–120 min o.v. 30 min Ic. 5–30 mg/L	[82]
CHAC CA-CHAC	Cu (II)	612.52 mg/g 643.92 mg/g	pH 3–7 o.v.7 2–6 mg o.v. 5 mg 15–75 min o.v. 45 min(CHAC) and 30 min (CA-CHAC) Ic. 5–45 mg/L	[62]
AC-Ag-SiO_2	Cu^{2+}, Pb^{2+}, Cd^{2+} Zn^{2+}	84.75 mg/g, 81.3 mg/g, 87.72 mg/g, 81.97 mg/g	pH 2–12 o.v. 5.5 0.1–0.4 g o.v. 0.1 g 0–280 min o.v. 200 min Ic. 10 mg/L to 100 mg/L	[16]

Table 5. *Cont.*

Activated Carbon	Adsorbate	q_{max}	Adsorption Parameters (pH, Contact Time, Adsorption Dose, Initial Concentration-Ic)	Reference
CCAK7 CCAKN7	U(VI)	46.32 mg/g 51.66 mg/g	pH 6 55 min Ic 20–100 ppm	[22]
CC-AC	Cr(VI) Ni(II)	28.90 mg/g 6.27 mg/g	pH 2,7 o.v. 2 0–140 min o.v. 105 min, 0.1–0.3 g/100 mL o.v. 0.289 g, Ic 20–140 ppm o.v.37.2 ppm Cr (VI) pH 7,12 o.v. 12, 0–260 min o.v. 135 min, 0.2–1 g/100 mL o.v.0.94 g, Ic 20–100 ppm o.v.31 ppm Ni (II)	[64]

5.5. Impact of Temperature and Thermodynamic Studies

The effect of temperature on adsorption processes is commonly evaluated through thermodynamic parameters, including changes in Gibbs free energy (ΔG^0), enthalpy (ΔH^0), and entropy (ΔS^0). The magnitudes of ΔG^0, ΔH^0, and ΔS^0 are very important; a negative value of ΔG^0 for all metal ions adsorbed indicates that the adsorption process was spontaneous and favorable, and the positive entropy ΔS^0 value suggests that randomness increased in the adsorption system [50,83]. The enthalpy change (ΔH^0) is a useful indicator for distinguishing between physical and chemical adsorption. Typically, the enthalpy of physical adsorption does not exceed 4 kJ/mol, whereas for chemical adsorption it is generally higher than 20 kJ/mol [60]. Silvia et al. studied the thermodynamic behavior of Pb^{2+} and Cu^{2+} adsorption on activated carbon fibers (ACF). They analyzed parameters such as ΔG^0, ΔH^0, and ΔS^0 to evaluate the spontaneity of the adsorption. The negative ΔG^0 values indicated that adsorption was spontaneous, and the positive ΔH^0 values showed that the processes were endothermic. The ΔH^0 magnitudes (23.39 kJ/mol for Cu^{2+} and 53.94 kJ/mol for Pb^{2+}) suggested that chemisorption was the main mechanism. Additionally, positive ΔS^0 values reflected increased disorder at the adsorbent–adsorbate interface, pointing to the possible reversible interactions [58]. Bozbeyoğlu et al. emphasized that temperature is a key factor affecting the adsorption process, as it determines how efficiently the system performs under different environmental conditions and how closely its behavior approaches that observed under laboratory settings. To evaluate this effect, they studied the adsorption of Cr(VI) onto CCs-AC within a temperature range of 5–50 °C. The ΔG values became more negative with increasing temperature, confirming that the adsorption was spontaneous and thermodynamically more favorable at higher temperatures. At lower Cr(VI) concentrations, room temperature was sufficient to achieve spontaneous adsorption, while at higher concentrations (250 mg/L), elevated temperatures further enhanced adsorption feasibility. The positive enthalpy change (ΔH^0 = 12.0 kJ/mol) indicated that the process was endothermic and suggested that adsorption was slightly chemical rather than physical interaction. Moreover, the positive entropy value (ΔS^0 = 40.69 J/molK) reflected an increase in randomness at the solid–liquid interface, implying greater mobility and disorder of Cr(VI) ions during adsorption on the CCs-AC surface [60]. Giraldo et al. conducted a thermodynamic study to evaluate the effect of temperature on the adsorption of U(VI) ions onto three activated carbon samples prepared from corncob, namely the nitrogen-doped activated carbon (CCAKN7), activated carbon material (CCAK7), and carbonized corn carbon (CC). The obtained thermodynamic parameters (ΔG^0, ΔH^0, and ΔS^0) revealed that the adsorption process was spontaneous and involved physisorption and chemical contributions. The ΔG^0 values ranged from −41.66 to −21.32 kJ/mol, confirming the spontaneity of the adsorption process. The enthalpy change (ΔH^0) values were −94.65 kJ/mol

for CCAKN7, −65.34 kJ/mol for CCAK7, and −52.81 kJ/mol for CC, indicating that the adsorption was exothermic and suggesting a combination of physical adsorption enhanced by chemical interactions. The negative entropy changes (ΔS^0) obtained for all samples indicated a decrease in randomness at the solid–liquid interface, implying structural ordering during adsorption [22]. Thermodynamic parameters for activated carbon materials derived from corn waste are summarized in Table 6. The results indicate that the adsorption of heavy metal ions onto activated carbon derived from corn waste is predominantly endothermic, with ΔH^0 values mostly positive. Adsorption efficiency generally improves with increasing temperature. Negative ΔG^0 values across all systems confirm that the process is spontaneous. Positive ΔS^0 values suggest increased randomness at the solid-solution interface, reflecting the replacement of water molecules and reorganization of ions on the adsorbent surface. Occasional negative ΔH^0 values indicate that exothermic chemisorptive interactions may occur under certain conditions, highlighting the presence of active sites with different binding energies. Overall, these results show that adsorption is temperature-dependent, spontaneous, and driven by a combination of physical and chemical interactions, although behavior may vary depending on the type of metal ion and experimental conditions.

Table 6. Thermodynamic parameters for the adsorption of heavy metals onto activated carbon materials from corn waste.

Adsorbent	Adsorbate	Temperature	ΔG^0 (kJ/mol)	ΔH^0 (kJ/mol)	ΔS^0	Reference
ACF	Pb^{2+}, Cu^{2+}	303 K 313 K 323 K 333 K	−26.12 Pb^{2+}, −22.03 Cu^{2+} −29.28 Pb^{2+}, −23.33 Cu^{2+} −31.78 Pb^{2+} −25.66 Cu^{2+} −34.08 Pb^{2+} −26.23 Cu^{2+}	53.94 Pb^{2+} 23.39 Cu^{2+}	264.87 J/mol K Pb^{2+} 149.96 J/mol K Cu^{2+}	[58]
CCs-AC	Cr (VI)	5 °C 15 °C 25 °C 35 °C 50 °C	0.85 0.18 −0.26 −0.62 −1.85	12 kJ/mol	40.69 J/mol K	[60]
Carbon derived from corn straw	Cr (VI)	298 K 313 K 328 K	−2.42 −3.57 −4.86	21.70 kJ/mol	0.08 kJ/mol K	[15]
CCAC	Cr (VI)	288 K 293 K 298 K 303 K 308 K	−1.929 −1.663 −1.805 −1.843 −1.710	6.6875 kJ/mol	6.5913 J/mol K	[61]
CAC AL-CAC	Fe (III)	35 °C 40 °C 45 °C	−32.33, −26.47 (CAC, AL-CAC) −33.12, −27.08 (CAC, AL-CAC) −34.05, −27.85 (CAC, AL-CAC)	−3.03 (CAC) −6.56 (AL-CAC)	81.51 J/mol K (CAC) 90.37 J/mol K (AL-CAC)	[18]

Table 6. *Cont.*

Adsorbent	Adsorbate	Temperature	ΔG^0 (kJ/mol)	ΔH^0 (kJ/mol)	ΔS^0	Reference
CS-C	Cd (II)	25 °C 30 °C 40 °C 50 °C	−17.48 −17.97 −19.57 −21.12	26.83	148.7 J/mol K	[79]
AC-Ag-SiO_2	Cu^{2+}, Pb^{2+}, Cd^{2+}, Zn^{2+}	298 K	−6.85 Cu^{2+} −11.62 Pb^{2+} −5.45 Cd^{2+} −8.72 Zn^{2+}	30.24 Cu^{2+}	123.6 J/mol K Cu^{2+}	[16]
		308 K	−7.53 Cu^{2+} −11.36 Pb^{2+} −6.57 Cd^{2+} −11.69 Zn^{2+}	25.89 Pb^{2+}	126.4 J/mol K Pb^{2+}	
		318 K	−8.87 Cu^{2+} −14.10 Pb^{2+} −7.59 Cd^{2+} −12.68 Zn^{2+}	22.81 Cd^{2+}	95.1 J/mol K Cd^{2+}	
		328 K	−10.57 Cu^{2+} −15.57 Pb^{2+} −8.26 Cd^{2+} −13.72 Zn^{2+}	39.12 Zn^{2+}	162.4 J/mol K Zn^{2+}	
CCAKN7	U(VI)	298 K 303 K 308 K 313 K	–32.45 −37.75 −39.84 −41.66	−94.65	−158.32 J/mol K	[22]
CCAK7		298 K 303 K 308 K 313 K	–32.38 −28.34 −26.32 –23.45	−65.34	−94.57 J/mol K	
CC		298 K 303 K 308 K 313 K	−30.21 −28.12 −24.37 −21.32	−52.81	−77.34 J/mol K	

6. Mechanism of Heavy Metal Removal Using Corn Waste–Based Carbon Material

The removal efficiency of heavy metal ions depends strongly on the chemical speciation of the metal and the structural and surface properties of the adsorbent, such as porosity, surface area, and functional groups present on the surface of activated carbon [79]. Although the adsorption of heavy metals has been extensively studied, most of the research has primarily focused on isotherm models, kinetic parameters, and thermodynamic evaluations. Nevertheless, while these models are valuable for estimating adsorption capacity and describing system behavior [84], they provide limited insight into the underlying adsorption mechanisms. Reliable conclusions about these interactions require detailed structural and chemical characterization of adsorbents before and after adsorption. A comprehensive understanding of the adsorption mechanism requires the application of advanced techniques, including BET surface area analysis, zeta potential measurements, cation exchange capacity (CEC), FTIR, XPS [85]. Figure 3 illustrates the possible adsorption mechanisms between corn waste-derived activated carbon and heavy metal ions, including ion exchange, surface complexation, electrostatic interaction, physical adsorption, co-precipitation, and metal-π interaction, providing a clear visual summary of the

processes discussed throughout this review. Several studies have explored these mechanisms in carbon materials derived from corn waste. For example, Abou-Hadid et al. reported the cadmium adsorption mechanism on carbon species synthesized from corn shells. Their study revealed that the process is primarily controlled by inner-sphere surface complexation, where cadmium ions chemically interact with oxygen-containing functional groups such as –OH, –COOH, and –ROH. This mechanism was supported by FTIR analysis, which confirmed the presence of these reactive groups, and by kinetic modeling, where the pseudo-second-order model indicated chemisorption. Additionally, negative zeta potential values across the studied pH range suggested a secondary contribution of electrostatic attraction. As adsorption progressed and active sites became saturated, intraparticle diffusion became the rate-limiting step, as demonstrated by the Weber–Morris model. Additionally, BET surface area and porosity measurements showed that physical adsorption also played a supportive role in cadmium uptake, although chemical surface complexation remained the main mechanism [79]. Ma et al. investigated Cr(VI) removal using porous carbon derived from corn straw. The main mechanisms involved are ion exchange between Cr(VI) ions and surface carboxyl (–COOH) groups, complexation with hydroxyl and carbonyl groups, and partial reduction of Cr(VI) to Cr(III) facilitated by electron-donating groups on the carbon surface. The synergy of these processes resulted in efficient chromium removal [15]. Iamsaard et al. investigated Cu(II) adsorption on biochar derived from various agricultural wastes, including corn residues. For corn-derived biochar, the dominant removal mechanism was surface complexation between Cu(II) ions and oxygen-containing functional groups. XPS analysis revealed binding energy shifts in the C–O (532.2 to 533.0 eV) and C=O (530.7 to 531.9 eV) regions, confirming these interactions. Cation exchange also contributed, as Cu(II) displaced exchangeable cations originally bound to surface groups. Additionally, electrostatic attraction enhanced adsorption at pH values above the point of zero charge (pH_{pzc}), although surface complexation remained the predominant mechanism [80]. Tahir and Heryanto investigated the use of activated carbon derived from corn stalks for Pb(II) removal, with a particular emphasis on the implementation of IoT technology for real-time monitoring to obtain immediate feedback on changes in key adsorption parameters. The study identified several adsorption mechanisms: physical adsorption, complexation, electron transfer, and ion exchange. FTIR spectra revealed the presence of functional groups such as carbonyl (C=O), hydroxyl (O–H), and aromatic structures (C=C), indicating favorable surface chemistry for complexation. Electron transfer between Pb(II) and the adsorbent enhanced electrostatic interactions, while ion exchange occurred as Pb(II) replaced cations like Na^+ or K^+ bound to surface groups like C=O and O–H. Among these, complexation with carbonyl and hydroxyl groups was identified as the dominant adsorption mechanism [86]. It is important to highlight that some studies referenced in this review (e.g., [15,80]) involve biochar or porous carbon materials, which differ considerably from activated carbon in surface chemistry and pore structure. Therefore, research on activated carbon derived from corn waste should prioritize detailed investigation of adsorption mechanisms, employing comprehensive characterization techniques to better understand adsorption mechanisms and improve heavy metal removal performance.

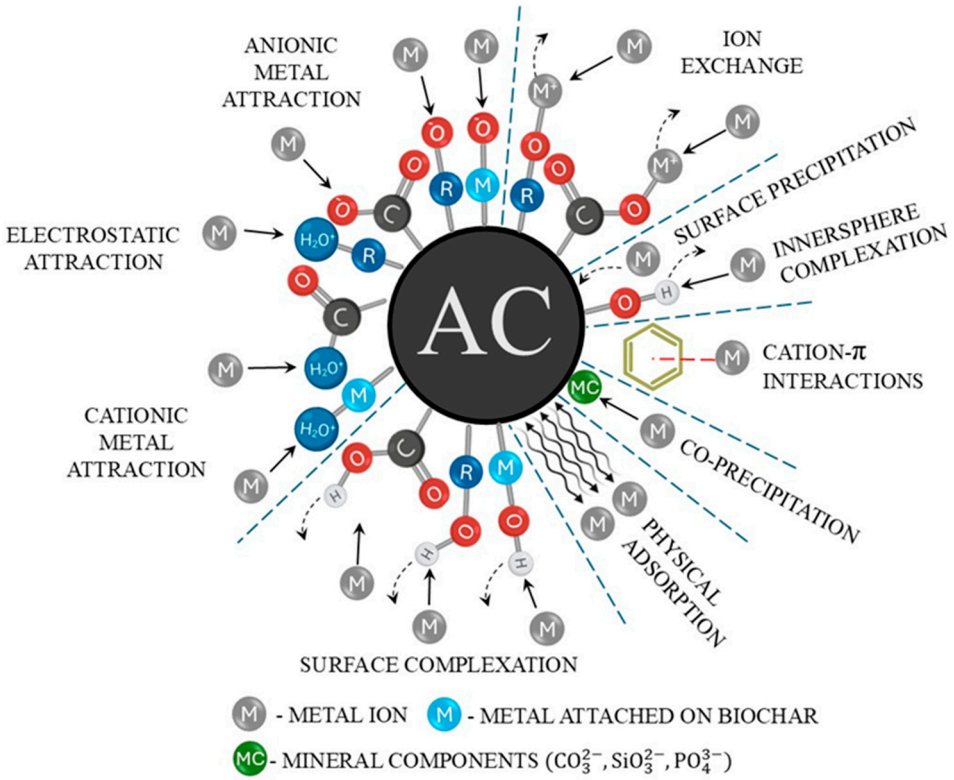


Figure 3. Possible adsorption mechanisms of heavy metal ions on activated carbon from corn residues.

7. Conclusions and Future Perspectives

This review highlights the significant potential of corn waste-derived activated carbon materials as effective and sustainable adsorbents for environmental applications. Activated carbon produced from corn residues has demonstrated high efficiency in removing various heavy metals from contaminated water and wastewater. To contextualize the adsorption performance, it is important to report the experimentally observed range of maximum adsorption capacities (0.19–643.92 mg/g) for individual metal ions, emphasizing the minimum and maximum values achieved. A comprehensive discussion is provided on the use of corn waste biomass to produce activated carbon, covering key aspects such as preparation and characterization methods, physicochemical properties, adsorption capacity for heavy metals, and primary mechanisms, thereby offering a solid basis for future investigations. Among corn residues, cobs are the most practical and widely investigated precursors due to their favorable lignocellulosic composition and centralized availability during post-harvest processing. Other residues, such as husks, tassels, and silk, although less explored, hold considerable potential for high-performance adsorbent production owing to their abundance and unique physicochemical characteristics. Future research should assess the economic feasibility of corn waste-derived adsorbents. Strategies such as combining different corn residues (stalks, husks, tassels, cobs, silk) or co-blending with other biomass or waste materials may enhance adsorption efficiency, reduce production costs, and support sustainable circular waste management. Furthermore, future studies should prioritize the evaluation of adsorption performance under real-world conditions, including the use of real wastewater samples, dynamic column systems, and complex multi-component solutions. Moreover, comprehensive optimization is necessary, considering a broad range of influencing parameters such as adsorbent dosage, pH, contact time, initial metal concentration, and thermodynamic behavior should be conducted using statistical approaches (e.g., response surface methodology). This would enable more accurate predictions of adsorption behavior and support scalable implementation. Detailed characterization remains crucial, with

emphasis on specific surface area and porosity, as these textural properties directly affect the number of active sites and metal ion accessibility. Understanding dominant interaction pathways, including ion exchange, surface complexation, and electrostatic attractions, is essential for guiding adsorbent design and tailoring materials for targeted environmental applications. A thorough understanding of adsorption mechanisms further supports the translation of laboratory-scale findings into practical, real-world solutions.

Author Contributions: M.R. conducted the literature review and wrote the manuscript; M.K., V.R., M.T. and M.M. contributed to the concept and reviewed the manuscript; S.Ž. supervised and checked the final document. All authors have read and agreed to the published version of the manuscript.

Funding: This research was funded by the Ministry of Science, Technological Development and Innovation of the Republic of Serbia (Contract number: 451-03-136/2025-03/200017).

Data Availability Statement: Not applicable.

Conflicts of Interest: The authors declare no conflicts of interest. The funders had no role in the design of the study; in the collection, analyses, or interpretation of data; in the writing of the manuscript; or in the decision to publish the results.

References

1. Younas, F.; Younas, S.; Bibi, I.; Farooqi, Z.U.R.; Hameed, M.A.; Mohy-Ud-Din, W.; Shehzad, M.T.; Hussain, M.M.; Shakil, Q.; Shahid, M.; et al. A critical review on the separation of heavy metal(loid)s from the contaminated water using various agricultural wastes. *Int. J. Phytoremediat.* **2024**, *26*, 349–368. [CrossRef]
2. Sherlala, A.I.A.; Raman, A.A.A.; Bello, M.M.; Asghar, A. A review of the applications of organo-functionalized magnetic graphene oxide nanocomposites for heavy metal adsorption. *Chemosphere* **2018**, *193*, 1004–1017. [CrossRef]
3. Hoang, A.T.; Kumar, S.; Lichtfouse, E.; Cheng, C.K.; Varma, R.S.; Senthilkumar, N.; Phong Nguyen, P.Q.; Nguyen, X.P. Remediation of heavy metal polluted waters using activated carbon from lignocellulosic biomass: An update of recent trends. *Chemosphere* **2022**, *302*, 134825. [CrossRef]
4. Uddin, M.K. A review on the adsorption of heavy metals by clay minerals, with special focus on the past decade. *Chem. Eng. J.* **2017**, *308*, 438–462. [CrossRef]
5. Burakov, A.E.; Galunin, E.V.; Burakova, I.V.; Kucherova, A.E.; Agarwal, S.; Tkachev, A.G.; Gupta, V.K. Adsorption of heavy metals on conventional and nanostructured materials for wastewater treatment purposes: A review. *Ecotoxicol. Environ. Saf.* **2018**, *148*, 702–712. [CrossRef]
6. Carolin, C.F.; Kumar, P.S.; Saravanan, A.; Joshiba, G.J.; Naushad, M. Efficient techniques for the removal of toxic heavy metals from aquatic environment: A review. *J. Environ. Chem. Eng.* **2017**, *5*, 2782–2799. [CrossRef]
7. Hou, X.-X.; Deng, Q.-F.; Ren, T.-Z.; Yuan, Z.-Y. Adsorption of Cu^{2+} and methyl orange from aqueous solutions by activated carbons of corncob-derived char wastes. *Environ. Sci. Pollut. Res.* **2013**, *20*, 8521–8534. [CrossRef] [PubMed]
8. Gundogdu, A.; Bozbeyoglu, P.; Imamoglu, M.; Baltaci, C.; Duran, C.; Bulut, V.N. Characterization of the Adsorption Mechanism of Cadmium(II) and Methylene Blue upon Corncobs Activated Carbon. *Anal. Lett.* **2023**, *56*, 433–448. [CrossRef]
9. Tan, G.; Mao, Y.; Wang, H.; Xu, N. A comparative study of arsenic(V), tetracycline and nitrate ions adsorption onto magnetic biochars and activated carbon. *Chem. Eng. Res. Des.* **2020**, *159*, 582–591. [CrossRef]
10. World Health Organization. *Guidelines for Drinking-Water Quality: Fourth Edition Incorporating the First and Second Addenda*; World Health Organization: Geneva, Switzerland, 1984; ISBN 9789240045064.
11. Bayuo, J.; Rwiza, M.J.; Mtei, K.M. Modeling and optimization of trivalent arsenic removal from wastewater using activated carbon produced from maize plant biomass: A multivariate experimental design approach. *Biomass Convers. Biorefin.* **2024**, *14*, 24809–24832. [CrossRef]
12. Abdel-Shafy, H.; Hefny, M.; Ahmed, H.M.; Abdel-Haleem, F. Removal of Cadmium, Nickel, and Zinc from aqueous solutions by activated carbon prepared from corncob—Waste agricultural materials. *Egypt. J. Chem.* **2021**, *65*, 677–687. [CrossRef]
13. Kwikima, M.M.; Mateso, S.; Chebude, Y. Potentials of agricultural wastes as the ultimate alternative adsorbent for cadmium removal from wastewater. A review. *Sci. Afr.* **2021**, *13*, e00934. [CrossRef]
14. Nethaji, S.; Sivasamy, A.; Mandal, A.B. Preparation and characterization of corn cob activated carbon coated with nano-sized magnetite particles for the removal of Cr(VI). *Bioresour. Technol.* **2013**, *134*, 94–100. [CrossRef]
15. Ma, H.; Yang, J.; Gao, X.; Liu, Z.; Liu, X.; Xu, Z. Removal of chromium (VI) from water by porous carbon derived from corn straw: Influencing factors, regeneration and mechanism. *J. Hazard. Mater.* **2019**, *369*, 550–560. [CrossRef]

16. Nyirenda, J.; Kalaba, G.; Munyati, O. Synthesis and characterization of an activated carbon-supported silver-silica nanocomposite for adsorption of heavy metal ions from water. *Results Eng.* **2022**, *15*, 100553. [CrossRef]
17. Liu, Z.; Sun, Y.; Xu, X.; Meng, X.; Qu, J.; Wang, Z.; Liu, C.; Qu, B. Preparation, characterization and application of activated carbon from corn cob by KOH activation for removal of Hg(II) from aqueous solution. *Bioresour. Technol.* **2020**, *306*, 123154. [CrossRef] [PubMed]
18. El-Bendary, N.; El-Etriby, H.K.; Mahanna, H. High-performance removal of iron from aqueous solution using modified activated carbon prepared from corn cobs and luffa sponge. *Desalination Water Treat.* **2021**, *213*, 348–357. [CrossRef]
19. Ermadani; Viviani, A.; Yasdi; Yanopa, S.; Suryanto; Arsyad, A.; Sarman. The use of activated charcoal from corn cobs as adsorbent of heavy metals from groundwater. *Rev. Bras. Eng. Biossistemas* **2023**, *17*, 1191. [CrossRef]
20. Lala, M.A.; Olomowewe, Z.O.; Adeniyi, A.T.; Giwa, A. Maize cob-derived activated carbon as an adsorbent for the removal of nickel (II) cation from aqueous solution: Optimization and kinetic studies. *Arab. J. Basic Appl. Sci.* **2023**, *30*, 573–582. [CrossRef]
21. Kouassi, N.L.B.; N'goran, K.P.D.A.; Blonde, L.D.; Diabate, D.; Albert, T. Simultaneous Removal of Copper and Lead from Industrial Effluents Using Corn Cob Activated Carbon. *Chem. Afr.* **2023**, *6*, 733–745. [CrossRef]
22. Giraldo, L.; Serafin, J.; Dziejarski, B.; Moreno-Piraján, J.C. Activated carbon from biomass waste as potential materials for uranium removal. *Chem. Eng. Sci.* **2025**, *306*, 121222. [CrossRef]
23. Zhang, Y.; Duan, X. Chemical precipitation of heavy metals from wastewater by using the synthetical magnesium hydroxy carbonate. *Water Sci. Technol.* **2020**, *81*, 1130–1136. [CrossRef]
24. Islamoglu, S.; Yilmaz, L.; Ozbelge, H.O. Development of a Precipitation Based Separation Scheme for Selective Removal and Recovery of Heavy Metals from Cadmium Rich Electroplating Industry Effluents. *Sep. Sci. Technol.* **2006**, *41*, 3367–3385. [CrossRef]
25. Lupa, L.; Cocheci, L. Heavy Metals Removal from Water and Wastewater. In *Heavy Metals—Recent Advances*; IntechOpen: London, UK, 2023. [CrossRef]
26. Al-Enezi, G.; Hamoda, M.F.; Fawzi, N. Ion Exchange Extraction of Heavy Metals from Wastewater Sludges. *J. Environ. Sci. Health Part A* **2004**, *39*, 455–464. [CrossRef]
27. Twizerimana, P.; Wu, Y. Overview of integrated electrocoagulation-adsorption strategies for the removal of heavy metal pollutants from wastewater. *Discov. Chem. Eng.* **2024**, *4*, 14. [CrossRef]
28. AlJaberi, F.Y. Operating cost analysis of a concentric aluminum tubes electrodes electrocoagulation reactor. *Heliyon* **2019**, *5*, e02307. [CrossRef] [PubMed]
29. Vidu, R.; Matei, E.; Predescu, A.M.; Alhalaili, B.; Pantilimon, C.; Tarcea, C.; Predescu, C. Removal of Heavy Metals from Wastewaters: A Challenge from Current Treatment Methods to Nanotechnology Applications. *Toxics* **2020**, *8*, 101. [CrossRef]
30. Zhao, G.; Chen, W.N. Biofouling formation and structure on original and modified PVDF membranes: Role of microbial species and membrane properties. *RSC Adv.* **2017**, *7*, 37990–38000. [CrossRef]
31. Othman, N.H.; Alias, N.H.; Fuzil, N.S.; Marpani, F.; Shahruddin, M.Z.; Chew, C.M.; David Ng, K.M.; Lau, W.J.; Ismail, A.F. A Review on the Use of Membrane Technology Systems in Developing Countries. *Membranes* **2021**, *12*, 30. [CrossRef]
32. Deischter, J.; Wolter, N.; Palkovits, R. Tailoring Activated Carbons for Efficient Downstream Processing: Selective Liquid-Phase Adsorption of Lysine. *ChemSusChem* **2020**, *13*, 3614–3621. [CrossRef]
33. Sun, Z.; Wang, M.; Fan, J.; Zhou, Y.; Zhang, L. Regeneration Performance of Activated Carbon for Desulfurization. *Appl. Sci.* **2020**, *10*, 6107. [CrossRef]
34. Zhang, T.; Yang, Y.; Li, X.; Zhou, Z.; Wei, B. Ultrasonic–Thermal Regeneration of Spent Powdered Activated Carbon. *Sustainability* **2023**, *15*, 9060. [CrossRef]
35. Abdel daiem, M.M.; Rivera-Utrilla, J.; Sánchez-Polo, M.; Ocampo-Pérez, R. Single, competitive, and dynamic adsorption on activated carbon of compounds used as plasticizers and herbicides. *Sci. Total Environ.* **2015**, *537*, 335–342. [CrossRef]
36. Rodríguez-Reinoso, F. Activated Carbon and Adsorption. In *Encyclopedia of Materials: Science and Technology*; Elsevier: Amsterdam, The Netherlands, 2001; pp. 22–34. [CrossRef]
37. Lewoyehu, M. Comprehensive review on synthesis and application of activated carbon from agricultural residues for the remediation of venomous pollutants in wastewater. *J. Anal. Appl. Pyrolysis* **2021**, *159*, 105279. [CrossRef]
38. Radenković, M.; Petrović, J.; Pap, S.; Kalijadis, A.; Momčilović, M.; Krstulović, N.; Živković, S. Waste biomass derived highly-porous carbon material for toxic metal removal: Optimisation, mechanisms and environmental implications. *Chemosphere* **2024**, *347*, 140684. [CrossRef] [PubMed]
39. Yahya, M.A.; Al-Qodah, Z.; Ngah, C.W.Z. Agricultural bio-waste materials as potential sustainable precursors used for activated carbon production: A review. *Renew. Sustain. Energy Rev.* **2015**, *46*, 218–235. [CrossRef]
40. Christica, I.; Julia, R. Activated Carbon Utilization from Corn Cob (*Zea mays*) as a Heavy Metal Adsorbent in Industrial Waste. *Asian J. Pharm. Res. Dev.* **2018**, *6*, 1–4. [CrossRef]
41. Ahmed, M.J.; Danish, M.; Anastopoulos, I.; Iwuozor, K.O. Recent progress on corn (*Zea mays* L.)-based materials as raw, chemically modified, carbonaceous, and composite adsorbents for aquatic pollutants: A review. *J. Anal. Appl. Pyrolysis* **2023**, *172*, 106004. [CrossRef]

42. Czajkowski, Ł.; Wojcieszak, D.; Olek, W.; Przybył, J. Thermal properties of fractions of corn stover. *Constr. Build. Mater.* **2019**, *210*, 709–712. [CrossRef]
43. Zhong, X.; Yuan, R.; Zhang, B.; Wang, B.; Chu, Y.; Wang, Z. Full fractionation of cellulose, hemicellulose, and lignin in pith-leaf containing corn stover by one-step treatment using aqueous formic acid. *Ind. Crops Prod.* **2021**, *172*, 113962. [CrossRef]
44. Sun, Y.; Webley, P.A. Preparation of activated carbons from corncob with large specific surface area by a variety of chemical activators and their application in gas storage. *Chem. Eng. J.* **2010**, *162*, 883–892. [CrossRef]
45. Drané, M.; Zbair, M.; Hajjar-Garreau, S.; Josien, L.; Michelin, L.; Bennici, S.; Limousy, L. Unveiling the Potential of Corn Cob Biochar: Analysis of Microstructure and Composition with Emphasis on Interaction with NO_2. *Materials* **2023**, *17*, 159. [CrossRef]
46. Choi, J.Y.; Nam, J.; Yun, B.Y.; Kim, Y.U.; Kim, S. Utilization of corn cob, an essential agricultural residue difficult to disposal: Composite board manufactured improved thermal performance using microencapsulated PCM. *Ind. Crops Prod.* **2022**, *183*, 114931. [CrossRef]
47. Liu, Y.; Xu, X.; Qu, B.; Liu, X.; Yi, W.; Zhang, H. Study on Adsorption Properties of Modified Corn Cob Activated Carbon for Mercury Ion. *Energies* **2021**, *14*, 4483. [CrossRef]
48. Zhao, J.; Yu, L.; Ma, H.; Zhou, F.; Yang, K.; Wu, G. Corn stalk-based activated carbon synthesized by a novel activation method for high-performance adsorption of hexavalent chromium in aqueous solutions. *J. Colloid. Interface Sci.* **2020**, *578*, 650–659. [CrossRef]
49. Li, Y.; Li, Y.; Li, L.; Shi, X.; Wang, Z. Preparation and analysis of activated carbon from sewage sludge and corn stalk. *Adv. Powder Technol.* **2016**, *27*, 684–691. [CrossRef]
50. Ismail, M.S.; Yahya, M.D.; Auta, M.; Obayomi, K.S. Facile preparation of amine-functionalized corn husk derived activated carbon for effective removal of selected heavy metals from battery recycling wastewater. *Heliyon* **2022**, *8*, e09516. [CrossRef]
51. Olorundare, O.F.; Krause, R.W.M.; Okonkwo, J.O.; Mamba, B.B. Potential application of activated carbon from maize tassel for the removal of heavy metals in water. *Phys. Chem. Earth Parts A/B/C* **2012**, *50–52*, 104–110. [CrossRef]
52. Heidarinejad, Z.; Dehghani, M.H.; Heidari, M.; Javedan, G.; Ali, I.; Sillanpää, M. Methods for preparation and activation of activated carbon: A review. *Environ. Chem. Lett.* **2020**, *18*, 393–415. [CrossRef]
53. Latiff, M.F.P.M.; Abustan, I.; Ahmad, M.A.; Yahaya, N.K.E.M.; Khalid, A.M. Effect of preparation conditions of activated carbon prepared from corncob by CO_2 activation for removal of Cu (II) from aqueous solution. In Proceedings of the 1st International Conference on Advanced Science, Engineering and Technology, Penang, Malaysia, 21–22 December 2015; p. 030001. [CrossRef]
54. Speranza, G. The Role of Functionalization in the Applications of Carbon Materials: An Overview. *C* **2019**, *5*, 84. [CrossRef]
55. El-Shafey, E.I.; Ali, S.N.F.; Al-Busafi, S.; Al-Lawati, H.A.J. Preparation and characterization of surface functionalized activated carbons from date palm leaflets and application for methylene blue removal. *J. Environ. Chem. Eng.* **2016**, *4*, 2713–2724. [CrossRef]
56. Rao, V.D.; Raghutu, R.; Rao, K.S.; Kumar, R.; Padma, D.V.; Sastry, S.V.A.R. Efficient biosorption of cadmium ions from wastewater using iron oxide–maize shell activated bio-carbon nanocomposites. *Biomass Convers. Biorefin.* **2024**. [CrossRef]
57. Ammar, N.S.; Fathy, N.A.; Ibrahim, H.S.; Mousa, S.M. Micro-mesoporous modified activated carbon from corn husks for removal of hexavalent chromium ions. *Appl. Water Sci.* **2021**, *11*, 154. [CrossRef]
58. Silva, M.C.; Crespo, L.H.S.; Cazetta, A.L.; Silva, T.L.; Spessato, L.; Almeida, V.C. Activated carbon fibers of high surface area from corn husk: Mono and multicomponent adsorption studies of Pb^{2+} and Cu^{2+} ions from aqueous solution. *J. Mol. Liq.* **2024**, *405*, 124919. [CrossRef]
59. Campos, N.F.; Guedes, G.A.J.C.; Oliveira, L.P.S.; Gama, B.M.V.; Sales, D.C.S.; Rodríguez-Díaz, J.M.; Barbosa, C.M.B.M.; Duarte, M.M.M.B. Competitive adsorption between Cu^{2+} and Ni^{2+} on corn cob activated carbon and the difference of thermal effects on mono and bicomponent systems. *J. Environ. Chem. Eng.* **2020**, *8*, 104232. [CrossRef]
60. Bozbeyoglu, P.; Gündoğdu, A. Adsorption of hexavalent chromium from aqueous solution onto corn cobs—Activated carbon. *Turk. J. Anal. Chem.* **2023**, *5*, 107–117. [CrossRef]
61. Li, H.; Gao, P.; Cui, J.; Zhang, F.; Wang, F.; Cheng, J. Preparation and Cr(VI) removal performance of corncob activated carbon. *Environ. Sci. Pollut. Res.* **2018**, *25*, 20743–20755. [CrossRef]
62. Gamay, K.P.; Ongayo, G.D. From Waste to Resource: Assessing the Biosorption Efficiency of Citric Acid-Modified Activated Carbon from Corn (*Zea mays*) Husks in Aqueous Copper (II) Ion Solutions. *Int. J. Res. Innov. Appl. Sci.* **2024**, *IX*, 468–479. [CrossRef]
63. Adebayo, G.; Adegoke, H.; Jamiu, W.; Balogun, B.; Jimoh, A. Adsorption of Mn(II) and Co(II) ions from aqueous solution using Maize cob activated carbon: Kinetics and Thermodynamics Studies. *J. Appl. Sci. Environ. Manag.* **2016**, *19*, 737. [CrossRef]
64. Kamel, M.; Bastaweesy, A.M.; Hefny, R.A. Optimized Removal of Cr (VI) and Ni (II) From Wastewater Using Corncob-Derived Activated Carbon. *Water Air Soil Pollut.* **2025**, *236*, 93. [CrossRef]
65. Pellenz, L.; de Oliveira, C.R.S.; da Silva Júnior, A.H.; da Silva, L.J.S.; da Silva, L.; Ulson de Souza, A.A.; de Souza, S.M.d.A.G.U.; Borba, F.H.; da Silva, A. A comprehensive guide for characterization of adsorbent materials. *Sep. Purif. Technol.* **2023**, *305*, 122435. [CrossRef]
66. Bläker, C.; Muthmann, J.; Pasel, C.; Bathen, D. Characterization of Activated Carbon Adsorbents—State of the Art and Novel Approaches. *ChemBioEng Rev.* **2019**, *6*, 119–138. [CrossRef]

67. González-García, P. Activated carbon from lignocellulosics precursors: A review of the synthesis methods, characterization techniques and applications. *Renew. Sustain. Energy Rev.* **2018**, *82*, 1393–1414. [CrossRef]
68. Shafeeyan, M.S.; Daud, W.M.A.W.; Houshmand, A.; Shamiri, A. A review on surface modification of activated carbon for carbon dioxide adsorption. *J. Anal. Appl. Pyrolysis* **2010**, *89*, 143–151. [CrossRef]
69. Tang, S.; Chen, Y.; Xie, R.; Jiang, W.; Jiang, Y. Preparation of activated carbon from corn cob and its adsorption behavior on Cr(VI) removal. *Water Sci. Technol.* **2016**, *73*, 2654–2661. [CrossRef]
70. Ahmad, T.; Danish, M. A review of avocado waste-derived adsorbents: Characterizations, adsorption characteristics, and surface mechanism. *Chemosphere* **2022**, *296*, 134036. [CrossRef]
71. Cao, Q.; Xie, K.; Lv, Y.; Bao W. Process effects on activated carbon with large specific surface area from corn cob. *Bioresour. Technol.* **2006**, *97*, 110–115. [CrossRef]
72. Fiol, N.; Villaescusa, I. Determination of sorbent point zero charge: Usefulness in sorption studies. *Environ. Chem. Lett.* **2009**, *7*, 79–84. [CrossRef]
73. Julien, F.; Baudu, M.; Mazet, M. Relationship between chemical and physical surface properties of activated carbon. *Water Res.* **1998**, *32*, 3414–3424. [CrossRef]
74. Aliyu, S.; Salahudeen, N.; Rasheed, A.A. Adsorptive Removal of Lead (II) Pollutants from Wastewater Using Corncob-Activated Carbon. *J. Eng. Sci.* **2024**, *11*, H1–H10. [CrossRef]
75. El-Hendawy, A.-N.A. An insight into the KOH activation mechanism through the production of microporous activated carbon for the removal of Pb^{2+} cations. *Appl. Surf. Sci.* **2009**, *255*, 3723–3730. [CrossRef]
76. Duan, X.-L.; Yuan, C.-G.; Jing, T.-T.; Yuan, X.-D. Removal of elemental mercury using large surface area micro-porous corn cob activated carbon by zinc chloride activation. *Fuel* **2019**, *239*, 830–840. [CrossRef]
77. Ekinci, S.; Onat, E.; Atiç, S. Optimized Synthesis and Characterization of Activated Carbon from Corn Silk and Corn Silk Hydrochar. *ChemistrySelect* **2025**, *10*, e202405854. [CrossRef]
78. Anastopoulos, I.; Karamesouti, M.; Mitropoulos, A.C.; Kyzas, G.Z. A review for coffee adsorbents. *J. Mol. Liq.* **2017**, *229*, 555–565. [CrossRef]
79. Abou-Hadid, A.F.; El-Behairy, U.A.; Elmalih, M.M.; Amdeha, E.; El Naggar, A.M.A.; Taha, M.H.; Hussein, A.E.M. Conversion of corn shell as biomass solid waste into carbon species for efficient decontamination of wastewater via heavy metals adsorption. *Biomass Convers. Biorefin.* **2024**, *14*, 16435–16449. [CrossRef]
80. Iamsaard, K.; Weng, C.-H.; Tzeng, J.-H.; Anotai, J.; Jacobson, A.R.; Lin, Y.-T. Systematic optimization of biochars derived from corn wastes, pineapple leaf, and sugarcane bagasse for Cu(II) adsorption through response surface methodology. *Bioresour. Technol.* **2023**, *382*, 129131. [CrossRef] [PubMed]
81. Abas, S.N.; Ismail, M.H.; Kamal, L.M.; Izhar, S. Adsorption Process of Heavy Metals by Low-Cost Adsorbent: A Review. *World Appl. Sci. J.* **2013**, *28*, 1518–1530.
82. Nadeem, U. Adsorption of Pb(II) from aqueous solutions by activated carbon prepared from agricultural waste: Maize leaves. *Eur. Chem. Bull.* **2013**, *2*, 927–931.
83. Anastopoulos, I.; Ighalo, J.O.; Adaobi Igwegbe, C.; Giannakoudakis, D.A.; Triantafyllidis, K.S.; Pashalidis, I.; Kalderis, D. Sunflower-biomass derived adsorbents for toxic/heavy metals removal from (waste) water. *J. Mol. Liq.* **2021**, *342*, 117540. [CrossRef]
84. Chen, X.; Hossain, M.F.; Duan, C.; Lu, J.; Tsang, Y.F.; Islam, M.S.; Zhou, Y. Isotherm models for adsorption of heavy metals from water—A review. *Chemosphere* **2022**, *307*, 135545. [CrossRef]
85. Shahrokhi-Shahraki, R.; Benally, C.; El-Din, M.G.; Park, J. High efficiency removal of heavy metals using tire-derived activated carbon vs. commercial activated carbon: Insights into the adsorption mechanisms. *Chemosphere* **2021**, *264*, 128455. [CrossRef] [PubMed]
86. Tahir, D.; Heryanto, H. Novel corn stalks derived activated carbon for promising adsorption of lead (II) from aqueous solution: Characterization, IoT real-time monitoring, and performance investigation. *Surf. Interfaces* **2025**, *61*, 106138. [CrossRef]

Disclaimer/Publisher's Note: The statements, opinions and data contained in all publications are solely those of the individual author(s) and contributor(s) and not of MDPI and/or the editor(s). MDPI and/or the editor(s) disclaim responsibility for any injury to people or property resulting from any ideas, methods, instructions or products referred to in the content.